

This is the author's peer reviewed, accepted manuscript. However, the online version of record will be different from this version once it has been copyedited and typeset.
PLEASE CITE THIS ARTICLE AS DOI: 10.1063/5.0098011

Plasmas for in-situ resource utilization on Mars: fuels, life-support and agriculture

V. Guerra,^{1, a)} T. Silva,^{1, b)} N. Pinhão,¹ O. Guaitella,² C. Guerra-Garcia,³ F.J.J. Peeters,^{4, 5} M.N. Tsampas,⁵ and M.C.M. van de Sanden^{5, 6}

¹⁾*Instituto de Plasmas e Fusão Nuclear, Instituto Superior Técnico, Universidade de Lisboa, 1049-001 Lisboa, Portugal*

²⁾*LPP, CNRS, École Polytechnique, Sorbonne Université, Université Paris-Saclay, IP-Paris, 91128 Palaiseau, France*

³⁾*Department of Aeronautics and Astronautics, Massachusetts Institute of Technology, Cambridge, MA, USA*

⁴⁾*Department of Mechanical Engineering, Eindhoven University of Technology, The Netherlands*

⁵⁾*Dutch Institute for Fundamental Energy Research (DIFFER), Eindhoven, The Netherlands*

⁶⁾*Eindhoven Institute of Renewable Energy Systems, Eindhoven University of Technology, The Netherlands*

(Dated: 7 July 2022)

This is the author's peer reviewed, accepted manuscript. However, the online version of record will be different from this version once it has been copyedited and typeset.
PLEASE CITE THIS ARTICLE AS DOI: 10.1063/5.0098011

This work discusses the potential of combining non-thermal plasmas and conducting membranes for in-situ resource utilization (ISRU) on Mars. By converting different molecules directly from the Martian atmosphere, plasmas can create the necessary feed-stock and base chemicals for processing fuels, breathing oxygen, building materials and fertilizers. Different plasma sources operate according to different principles and are associated with distinct dominant physicochemical mechanisms. This diversity allows exploring different energy transfer pathways leading to CO₂ dissociation, including direct electron impact processes, plasma chemistry mediated by vibrationally and electronically excited states, and thermally-driven dissociation. The coupling of plasmas with membranes is still a technology under development, but a synergistic effect between plasma decomposition and oxygen permeation across conducting membranes is anticipated. The emerging technology is versatile, scalable, and has the potential to deliver high rates of production of molecules per kilogram of instrumentation sent to space. Therefore, it will likely play a very relevant role in future ISRU strategies.

PACS numbers: 52.77.-j, 52.20.-j, 96.30.Gc, 07.87.+v

a) vguerra@tecnico.ulisboa.pt

b) tiago.p.silva@tecnico.ulisboa.pt

I. INTRODUCTION

Spaceflight programs are ever expanding and prospects of humans colonizing space to become a multi-planetary species are on the horizon.¹⁻⁴ To open the solar system for human exploration and colonization, several ongoing and planned space missions target the Moon and Mars.⁵⁻¹⁵ Their goals vary from pure scientific research to the development of the technologies needed to live and work on another world. A landmark is NASA's Artemis III mission,¹⁵ that foresees landing humans on the surface of the Moon in 2024, the first astronauts to walk on the Moon in over 50 years.¹⁵ The long-term goals of the Artemis program are to establish the first sustained presence on the Moon and to use the knowledge acquired on and around the Moon to take the next giant leap: sending the first astronauts to Mars.

In-situ resource utilization (ISRU) is crucial in this endeavour. Harnessing of resources in the exploration site instead of bringing them from Earth builds towards the self-sufficiency of space-bases and missions, and reduces the logistics, expenses and risks to the crew. The highest-impact ISRU products that can be used early in human operations are mission consumables including propellants, fuel cell reactants, and life support commodities.¹⁶ This is also the case for Mars exploration, where, at least on a first phase, ISRU will most likely be limited to Mars atmosphere resources for mission-critical applications.¹⁶

The main component of the Martian atmosphere is carbon dioxide (95.9%), with smaller percentages of Ar (1.9%), N₂ (1.9%) and other gases. The abundant CO₂ can be converted directly from the atmosphere into oxygen (O₂) and carbon monoxide (CO). O₂ can then be collected and made available for breathing, feeding indoors environments. Portable breathing devices that directly convert CO₂ from the atmosphere into O₂, allowing astronauts to wander outside without the need of O₂ storage, can also be dreamed of. In addition, both CO and O₂ can be used in a propellant mixture in rocket vehicles.¹⁷ Decomposition can be further pursued to arrive at carbon (C), of use for in-situ manufacturing of carbon structures and for the synthesis of different organic molecules. Besides, this route doubles the oxygen production, albeit at an extra energy cost. Carbon is also a fertilizer¹⁸ and a carbon feedstock is required for future Martian agriculture. Nitrogen (N₂) is another constituent of the atmosphere of Mars of interest for ISRU. It is essential for life-support as a breathing gas and, once oxygen has been made available, can be used for the local production of NO_x for fertilizers.^{19,20}

The only concrete proposal for oxygen production on Mars to date is the MOXIE experiment,^{21–25} under the framework of the Mars 2020 (Perseverance) mission.²⁶ It is based on solid oxide electrolysis cells (SOECs), in which, under electric bias, electrode materials offer catalytically active sites for CO₂ reduction to CO and oxygen evolution reactions respectively, while the electrolyte provides the required pathway for transporting oxide ions from the cathode to the anode. MOXIE's SOEC operates at temperature above 1000 K and pressures in the range 260-760 Torr.²⁵ Despite being a readily available technology, SOEC has several technical downsides regarding CO₂ conversion. The difficulty to break the carbon-oxygen double bond poses challenging requirements on electrode materials. The most commonly used electrode material is based on Ni cermet that is susceptible to degradation under reduction oxidation cycles and carbon deposition, requiring protective CO atmosphere and operating conditions to maintain stable operation.^{27–29} Particularly under the Martian scenario, the need of high temperatures²⁷ calls for a careful design of the thermal insulation system; the process of collecting and compressing the thin atmosphere of Mars (about 160 times thinner than Earth's atmosphere) prior to the decomposition process impose a technological limit that calls for additional pumping equipment to compress the gas inside the reactor, increasing the mass and power requirements of the system.²⁵

A new and complementary approach is proposed here, linking two emerging technologies: non-thermal plasmas and conducting membranes. Non-thermal plasmas are highly-reactive gas media sustained by electrical discharges, that allow the coexistence of energetic electrons (> 1.5 eV) with relatively cold gas molecules. Under these conditions, far from thermodynamic equilibrium, the discharge power can be selectively channeled, offering unique ways to break the strong C=O bond by taking advantage of the energy stored in the internal degrees of freedom. The combination of plasma with oxygen separation membrane-based systems may rely on either pure oxygen ion conducting^{30,31} or mixed oxygen ion electron conducting^{32–34} membranes. Either way, the system allows a compact design and direct separation of the conversion products.

Other strong points in favour of plasma technologies are that they are compact, scalable, reliable, versatile, do not require the use of expensive materials, operate on (renewable) electricity and can be powered by solar panels and batteries, can instantaneously start and stop operation (being thus perfectly adapted to a power supply from intermittent renewable energy sources), and can operate directly under Martian conditions without the need for

compression (as the Martian pressure is ideal for plasma ignition³⁵) or external heating on the O₂ production step.

Non-thermal plasmas have gained much attention in the last decade in the context of climate change and CO₂ valorization on Earth, due to their potential to activate CO₂ at reduced energy cost.^{36–38} Dissociation of CO₂ is one of the critical steps on the way to produce green synthetic fuels and platform molecules for the chemical industry and has been the focus of many studies, exploring electron impact,^{39,40} vibrationally-driven^{41,42} and thermal dissociation routes.^{43–45} As an extension of the vast investigation addressing the production of solar fuels on Earth (see Pietanza *et al*⁴⁶ and George *et al*³⁸ and references therein), it was recently noted that the knowledge acquired on Earth can be transferred to some extent to ISRU on Mars.⁴⁷ The very strong case supporting plasma-based production of oxygen on Mars presented by Guerra *et al*⁴⁷ predicted theoretically that the Martian atmospheric conditions of pressure, temperature and gas composition, are very favourable to ignite a plasma system and to achieve efficient CO₂ decomposition under a non-thermal regime. It was further noted that the presence of Ar and N₂ from the Martian atmosphere contributes to further enhancing plasma dissociation, and that the required power for discharge operation is typically ~ 100 W and can be as low as ~ 20 W at gas flows in the range 2-10 sccm,^{48,49} perfectly attainable on Mars.

The feasibility of oxygen production on Mars using plasma technologies was subsequently corroborated in two experimental campaigns, carried out at Laboratoire de Physique des Plasmas, Ecole Polytechnique, France, and the Dutch Institute For Fundamental Energy Research (DIFFER). In the first campaign, a DC glow discharge was cooled down to Martian temperatures by inserting a plasma reactor inside a cold bath of dry ice and ethanol.⁴⁹ The cold Martian temperatures did increase the CO₂ vibrational degree on non-equilibrium, a beneficial effect of Ar and N₂ was observed, and the reactor provided dissociation fractions in the range of 10-30%. These results are very encouraging considering that the plasma setup used was designed for fundamental research and is far from suited to the development of a prototype. The second experimental campaign showed that microwave (MW) discharges, operating under Martian composition and pressure, can provide CO₂ conversions of about 35% for a power around 300 W and gas flow of 50 sccm,⁵⁰ bringing the plasma results to a very competitive standard.

The other piece required to produce mission consumables is the separation of the products

produced in the plasma. For pure oxygen ion-conducting membranes, the oxygen separation step may leverage on SOEC, using the same principle as in MOXIE. The plasma may be generated on top of the solid oxide membrane, to assist CO₂ conversion and thus relax electrode requirements. This configuration is expected to increase the flow of oxygen through the membrane, since the production of O atoms in a plasma is much larger than on the surface of a conventional cathode. Furthermore, it has enhanced durability and brings cost reduction. Yttria (or Scandia) Stabilized Zirconia YSZ (ScSZ) seem to be good candidates to be used in oxygen ion-conducting membrane. A heat integration is also possible in order to use the heat losses of plasma to heat the SOEC. Preliminary results, obtained in a DC hollow cathode discharge used to study O₂ separation in a plasma+YSZ reactor, show evidence of increased durability of the SOEC process when used with a plasma enhanced gas stream, observed already with a dissociated flow of CO₂/O₂/CO.³⁰ Furthermore, a synergistic effect due to the presence of electrical charge was also evinced by plasma exsolution of nanoparticles,³¹ which brings additional electro-catalytical pathways to improve the process.

A separation stage based on mixed ionic electronic conduction (MIEC) membranes is also to consider. MIEC membranes are less complex than SOEC, but require additional pumping, as the oxygen permeation is driven by its partial pressure gradient across the membrane.³²⁻³⁴ These membranes are also good candidates to benefit from plasma-assistance, since the plasma can enhance the surface exchange kinetics owing to the presence of free electrons and oxygen radicals, which lead to increased oxygen permeation fluxes.³³ Challenges associated with MIEC are their stability in CO₂ and the possibility of back reactions during operation (that lead to a reduction of the total permeation flux).

The preliminary results already obtained for plasma CO₂ dissociation in DC and MW discharges support the estimation that an optimized system may produce oxygen at a rate of 14 g/h using a 6 kg plasma reactor, amounting to 2.3 g of oxygen produced per hour per kg of equipment sent to Mars.^{49,50} These values are about 6 times larger than obtained by the current operation of MOXIE and are discussed in section V.

The structure of this paper is as follows. Section II describes the types of plasma reactors more commonly used in CO₂ conversion studies and their characteristics. Section III reviews the available solutions for O₂ separation and anticipates the strategy foreseen for a coupled plasma-membrane system. Section IV addresses the current status of plasma-chemistry in CO₂ plasmas, and brings new results and insight into the operation of low-temperature

plasmas in a synthetic Martian atmosphere. Section V gives an overview of the figures of merit for the perspective of using plasmas for in-situ resource utilization on Mars and how they compare with MOXIE, establishing the high potential of the emerging technology. Finally, section VI summarizes the main results, gives directions for future research and concludes the paper.

II. PLASMA REACTORS

Plasma reactors use an external electric field to generate and accelerate electrons, which then share their energy with the rest of the gas through electron-impact excitation, dissociation, and ionization collisions, creating a very reactive environment. This reactivity is of particular interest for CO₂ conversion, as CO₂ is a highly stable molecule which typically requires substantial energy input and active catalysts for chemical reactions to take place.⁵¹ From a practical perspective, important metrics of performance for plasma reactors are energy efficiency and conversion rate. From a fundamental perspective, plasma reactors can be classified in terms of their reduced electric field, E/N , where E is the electric field and N is the gas density; and electron density, n_e .³⁷ Here we part from the fundamental parameters and connect them to the observed or expected performance of different plasma reactors for CO₂ conversion.

The reduced electric field determines the average electron energy or electron “temperature,” which in turn dictates which electron-impact reactions are favored and how the energy is shared with the gas, as it is shown, e.g., in figure 1 of Grofulović *et al*⁵² and in figure 11 of Ogloblina *et al*.⁵³ The value of E/N in the discharge is closely related with the energy efficiency of the process. In gaseous CO₂, nonequilibrium conditions arise for $E/N > 1$ Td (1 Td is equivalent to 250 V applied across a 1 cm gap at standard pressure and temperature): beyond this value, electron temperatures greater than the temperature of the gas can be accessed and efficient energy pathways of CO₂ dissociation are favored.^{54,55} Between $E/N \sim 10 - 100$ Td, CO₂ dissociation mainly follows from electron impact excitation of low vibrational levels, $\mathcal{O}(0.1-1$ eV), which interact among themselves through vibrational-vibrational (V-V) energy exchange processes, climbing the vibrational ladder, and reaching energy levels that can result in dissociative quenching.⁵¹ Gliding arcs (GA), microwave (MW) discharges, and radio frequency (RF) discharges are different types of

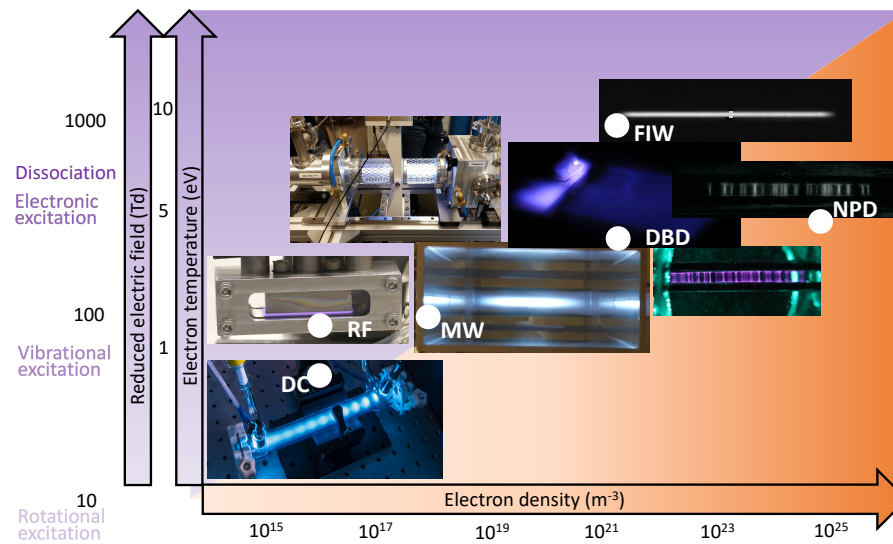


FIG. 1. Overview of different plasma sources and typical values of electron temperature, reduced electric field and electron density reached in their operation: CO₂ DC glow at 1mbar (photo credit: O. Guaitella),⁵⁷ 2% CO₂ in Argon RF plasma at 1 bar (photo credit: T. Gans, O. Guaitella), CO₂ MW plasma at 200 mbar - bottom image (photo credit: F. Peeters), CO₂ MW plasma at 7 mbar - top image (photo credit: T. Silva),⁵⁹ CO₂ surface DBD at 5 mbar (photo credit: O. Guaitella), CO₂/N₂ DBD plasma at 200 mbar (photo credit: O. Guaitella), postcombustion products NPD DBD plasma at 1 bar (photo credit: C. Pavan, C. Guerra-Garcia),⁶² CO₂ Fast Ionization Wave (FIW) inside a capillary tube at 10 mbar (photo credit: G. Pokrovskiy).^{60,63} All photos included with permission from the authors.

plasmas that can access this range of reduced electric fields, which explains why the literature on CO₂ conversion, seeking high energy efficiency, has greatly focused on these plasma sources.⁵⁶ Figure 1 summarizes the typical parameter space of operation of various types of discharges.^{57–61}

Early experiments with MW reactors report energy efficiencies of (80-90)%,³⁶ yet these typically require both low pressure $\mathcal{O}(100\text{mbar})$ and low temperature conditions so that vibrational-translational (V-T) relaxational processes and reverse oxidation of CO into carbon dioxide play a minor role.⁴⁶ In practice, these high efficiencies have not been reproduced in the past decade. It is now recognized that for GA, MW and RF plasmas, jointly referred to as warm plasmas, the gas temperature typically exceeds a few thousand kelvin and vibrational-translational (V-T) relaxation processes, as well as backward reactions, cannot

be neglected,⁶⁴ lowering the energy efficiency to the (40-60)% range.⁵¹ In these regimes, thermal dissociation in the discharge core has a dominant role and optimization of the post-discharge environment, rather than the plasma environment, offers most opportunities for improvement of the plasma-chemical conversion process, due to the importance of kinetics and turbulent transport in the cooling trajectory.^{44,45}

Below $E/N \sim 80$ Td the energy channeled to ionization in CO₂ plasmas is negligible compared with the energy spent in excitation, with the electron energy being essentially consumed in the excitation of the vibration levels.^{52,53} At $E/N > 100$ Td electron temperatures exceed a few eV and electronic excitation starts to dominate over the vibration modes,^{53,65} leading to higher-energy consumption channels of CO₂ dissociation. However, the higher degree of nonequilibrium, lower gas temperature, and higher ionization degree all favor higher conversion rates. So far, the most popular plasma operating in the high E/N regime has been the dielectric barrier discharge (DBD). DBDs are driven by AC voltage and at least one of the electrodes is covered by a dielectric to limit the current flow in every half cycle of operation. Despite its modest energy efficiencies, typically below 15%,⁵¹ the popularity of the DBD is justified by its operation at atmospheric pressure and room temperature, scalability, ease of operation, and reasonable dissociation yields of up to 40%.^{51,66}

The wrestle between dissociation yield and energy efficiency is apparent when considering the plasma power density,

$$P = \mathbf{j} \cdot \mathbf{E} = (en_e\mu_e\mathbf{E}) \cdot \mathbf{E} = en_eN(N\mu_e)(E/N)^2, \quad (1)$$

where \mathbf{j} is the current density, e the electron charge, and $\mu_e\mathbf{E}$ the electron drift velocity, with μ_e the electron mobility and $(N\mu_e)$ a function of E/N .⁵⁴ At high E/N ionization is favored, increasing the number of electron-impact reactions. For warm plasmas, the electron density can be increased by increasing the plasma power, yielding higher conversion rates at the expense of lower energy efficiencies, *e.g.*, the 90% efficiencies achieved in supersonic expanding CO₂ MW plasma yielded conversions around 5-10%.^{36,67}

Although the results with MW, RF, GA and DBD plasmas are already very promising, we believe that improvements are possible in terms of energy efficiency and/or conversion, through further engineering of the plasma sources. For instance, DBD reactors, which operate at low temperature, offer the possibility to incorporate catalyst materials in the plasma to control the selective production of value-added compounds when considering co-

reactants.³⁸ Finally, the question arises if an increased yield justifies a penalty on energy efficiency, for reasonable power consumption. In particular, it should be kept in mind that an increased dissociation facilitates the process of separation of the products through the membrane (see section III) and that an energy balance for the overall process should be done, and not only for the plasma decomposition.

From this perspective, of particular interest is the excitation of the gas using ultra-short high-voltage pulses so that there is not enough time to significantly change the electron concentration.⁵⁴ Under such fast raising voltage pulses the gap can endure an over-voltage that is higher than the static breakdown condition,^{68,69} and high E/N , in the range of hundreds of Td, can be sustained. These energy pathways have proven to be extremely attractive in the related fields of Plasma-Assisted Combustion and Plasma-Assisted Ignition (PAC/PAI) by providing efficient energy deposition into electronic excitation.^{54,62,70} Experiments in air and nitrogen using Nanosecond Pulsed Discharges (NPD) have shown that electronic excitation by electron impact results in oxygen dissociation via collisions with electronically excited atoms and molecules,⁶⁷ and in fast gas heating, which is heat release by collisional relaxation of electronically excited species at rates faster than V-T relaxation, at rates around 50 K/ns at atmospheric pressure.^{67,71}

Recent experiments using fast ionization waves (FIW) in capillary tubes triggered by NPD operating at 10-20 mbar have confirmed that these mechanisms are also present in CO₂, in reactions of quenching of CO($a^3\Pi$), O(1S) and O(1D) metastable states at sub-microsecond timescales.^{60,63} FIW are an interesting regime of pulsed breakdown, reached for very high over-voltages.^{69,72} In the single pulse regime, energy efficiencies and dissociation fractions of around 20% were demonstrated, at reduced fields of 200-400 Td.^{60,63} More interestingly, the conversion fraction was increased to over 90% in a repetitively pulsed regime, $\mathcal{O}(100\text{ Hz}-1\text{ kHz})$.⁶³ Although the results are promising, the relative role of gas heating and dissociation following electronic excitation is not clear at present, as well as how these results will translate to NPD regimes at lower over-voltages, which appear more readily than FIW when using Nanosecond Repetitively Pulsed (NRP) discharges at kHz frequencies using pin-to-pin electrode configurations at atmospheric pressures and above.⁷²

Recent work at Centrale Supélec⁷³ and Università di Trento⁶¹ have addressed experiments of NRP in atmospheric pressure CO₂ using pin-to-pin electrode configurations. The experiments by Maillard *et al* used a very small electrode gap of 3 mm to generate a fully ionized

This is the author's peer reviewed, accepted manuscript. However, the online version of record will be different from this version once it has been copyedited and typeset.
PLEASE CITE THIS ARTICLE AS DOI: 10.1063/1.50098011

filament, despite the ns-pulsed voltage, with electron density in the order of 10^{18} cm⁻³ and measured temperatures of 30000 K.⁷³ This regime is very interesting as it yields reasonable electron temperatures and high electron number densities. The experiments by Ceppelli *et al* also observed the fully ionized regime using a similar 5 mm gap and pin-to-pin electrode setup.⁷⁴ They characterized the discharge in terms of the NRP voltage waveform, which typically displays multiple reflections due to mismatch of the impedance between the power supply and the variable-impedance plasma load, identified as two discharge types.⁶¹ The first one, on the first region, corresponds to breakdown, has relatively low charge density, high energy electron, requires high voltage for ignition and dissipates most of the discharge energy. The second type, characteristic of the consecutive temporal regions of the pulse, has a peak electron density of $\mathcal{O}(10^{18})$ cm⁻³, a low electron energy and requires much lower voltage to ignite, which corresponds to a spark and offers favorable conditions for vibrationally enhanced dissociation.⁶¹ Additional studies reveal a significant dependence of both conversion fraction and energy efficiency with the inter-pulse time. A burst mode (short inter-pulse times) was found to perform better than the continuous mode, for the same total energy, with maximum conversion (downstream) around 20% and maximum energy efficiency close to 60%.⁷⁵ Notice that the results on conversion exhibit a peak of dissociation around 70%,⁷⁴ that decays to the mentioned 20% during the afterglow. This suggests that an adequate quenching of the dissociation products in the afterglow may largely increase dissociation and energy efficiency, in line with the results in MW discharges.^{44,45}

Ultimately, more sophisticated electrical schemes can be devised by combining independent voltage waveforms to circumvent the otherwise limited degree of control over E/N and species generation. NRP/RF hybrid plasmas in molecular gases, namely nitrogen and its mixtures with H₂, CO, and CO₂, have recently demonstrated that selective electronic excitation of N₂ and ionization during the NRP waveform, followed by vibrational excitation of the ground electronic state molecules during the RF waveform, is indeed possible.⁷⁶ Considering the temporal waveforms of RF and NRP sources, this scheme can be sustained with a single pair of electrodes, so that the complexity of the reactor is not increased. The approach can also be extended to any reacting molecular gas mixture, to generate electronically excited molecules as well as atomic species (by the pulsed discharge) and vibrationally excited molecules (by the sub-breakdown RF discharge).⁷⁶ Other hybrid strategies have also been proposed, including: sub-breakdown RF fields + laser-induced plasmas to increase

the plasma volume compared to the laser-only strategy;⁷⁷ multi-frequency RF voltage waveforms to control the electron energy distribution function and therefore the plasma-produced chemical activity;⁷⁸ and DC + NRP plasmas to separately control the vibrational (low E/N) and electronic excitation (high E/N) in the discharge, respectively.⁷⁹⁻⁸¹ These results open the possibility of somewhat decoupling conversion rate and energy efficiency, and constitute a new and open field of research, that still requires further investigation. Eventually, hybrid plasmas might enable the optimization of the strategy to either maximize conversion rate, efficiency, or some combined figure of merit, in response to the mission's needs.

III. PRODUCT SEPARATION

Aside from sophisticated plasma excitation schemes to improve gas-phase conversion and efficiency, another path towards enhanced ISRU is the combination of plasma with (solid) membrane gas-separation methods. For the case of plasma operated in pure CO_2 , the products are always a mixture of CO_2 , CO and O_2 , necessitating a means of separating these products for further utilization. While conversion and separation can be detached from one another in time and space, synergistic effects can be expected to occur if the two are operated in tandem. Similar to introducing a catalytic surface into a DBD plasma to control product yields,^{82,83} an oxygen-permeable membrane bounding the plasma will naturally shift the equilibrium of the CO_2 dissociation reaction towards increased levels of CO and O .⁸⁴

Three types of oxygen permeable membranes can be distinguished:

- (i) Non-electrochemical membranes: materials that do not rely on charged species to achieve transport of oxygen, but are nonetheless selectively permeable to oxygen species. An example is silver, which has a high diffusion coefficient for atomic O , especially along grain boundaries.⁸⁵
- (ii) Mixed Ionic-Electronic Conductors (MIEC): materials which show electrical conductivity for both electrons and oxygen ions. Depending on the material and the operating conditions (*e.g.*, temperature and oxygen partial pressure), electrical conductivity between the two conducting species may vary significantly, but generally the conductivity of electrons is higher in perovskites. A broad variety of (ceramic) MIEC materials ex-

ist, showing oxygen ion conductivities in the range of 1-1000 S/m at $T > 1000$ K.³² Notice that conductivity can affect the surface reactions if any of the steps involve charge transfer.

- (iii) Pure oxygen ion conductors: materials which show electrical conductivity dominantly via oxygen ions moving between vacancies in the material. To be classified as a purely ionic conductor, the ionic conductivity σ_{ion} must be 2 orders of magnitude larger than the electronic conductivity σ_e .⁸⁶ Due to substantial energy barriers for diffusion of atoms through the lattice, significant electrical conductivity requires high operating temperatures. Yttria or Scandia Stabilized Zirconia (YSZ, ScSZ) are O^{2-} conductors at 0.1-1 S/m at temperatures of $T \simeq 1000$ K.⁸⁶

Of the above, ionic conductors must be part of a circuit to allow for continuous transport of oxygen. Mixed conductors and non-electrochemical membranes allow for continuous oxygen transport solely by ensuring that an O_2 concentration gradient is present between both sides of a membrane (which is the case under normal operation conditions and can be achieved using inert gas to sweep away the oxygen, using vacuum, or fuels to consume oxygen^{32,87}).

The oxygen separation based on the diffusion mechanism through either (i) oxygen ionic conductor systems integrating a Solid Oxide Electrolysis Cell (SOEC) or (ii) MIEC involves several sequential steps (under conventional conditions, *i.e.* absence of plasma). The driving force for the case of SOEC is the electric bias across the two electrodes (that are deposited on both sides of a pure oxygen ion conducting membrane) while for the case of MIEC is the partial pressure difference between the feed and permeate side.⁸⁸⁻⁹⁰ The typical sequential steps are depicted in Figure 2 and can be summarized as follows:

1. Bulk-to-surface mass transfer of gaseous oxygen (feed side to the membrane surface).
2. Dissociation (surface exchange). The oxygen molecule is adsorbed on the (i) SOEC electrode or (ii) MIEC membrane surface and dissociates catalytically first to oxygen atoms and then in oxygen ions (O^{2-}). On the feed side, this can be expressed, using the Kröger-Vink notation, as $1/2O_2 + 2e^- + V_{\circ}^{\bullet\bullet} \rightarrow O_{\circ}^X$, where $V_{\circ}^{\bullet\bullet}$ refers to oxygen vacancies in the membrane of the SOEC or MIEC and O_{\circ}^X to oxygen ions (O^{2-}) occupying the oxygen lattice.
3. Ionic transport (bulk diffusion). The oxygen ions diffuse through the membrane lattice

(mainly oxygen vacancies, but also other defects) under (i) electric bias for the case of SOEC and (ii) a pressure gradient between the feed and permeate side for the case of MIEC. To maintain electrical neutrality, electrons are transported at the same time in the opposite direction via (i) the external SOEC electrical circuit and through the electrode, and (ii) the MIEC membrane.

4. Association (surface exchange). The oxygen ions recombine to form oxygen molecules and desorb from the surface of the membrane. The reaction involved in this step is the opposite of step 2.
5. Surface-to-bulk mass transfer. Adsorbed oxygen on the SOEC electrode or MIEC membrane surface is desorbed to gaseous oxygen in the permeate side.

For the case of plasma activated Mars atmosphere gases the feed is quite exotic, so the separation process can be more complex. On the one hand, the feed side contains many “flavors” of oxygen (molecular, atomic, ions) that can accelerate the oxygen separation bypassing few of the aforementioned steps.⁹¹ For instance, oxygen ions generated on plasma and reaching the membrane can continue the separation from step 3. On the other hand, the feed side under plasma activation has other active species that can hinder the separation via back reactions like $\text{CO} + 1/2\text{O}_2$ or $\text{O} \rightarrow \text{CO}_2$.

For a non-electrochemical membrane, the flux ϕ_i of species i through a section of membrane at depth x can be written as:

$$\Phi_i(x) = D_i(x) \frac{\partial n_i(x)}{\partial x} \quad (2)$$

with D_i the diffusion coefficient for species i , and n_i its concentration. For a constant D_i over a membrane of thickness d , the steady-state flux reduces to:

$$\Phi_i = \frac{D_i}{d} (n_i^{\leftarrow} - n_i^{\rightarrow}), \quad (3)$$

with n_i^{\leftarrow} , n_i^{\rightarrow} the concentration of species i on either side of the membrane.

For electrochemical membranes, a charged species i with electrical mobility μ_i is subject to a different driving force, the electric field E :

$$\Phi_i(x) = \mu_i(x) E(x) n_i(x) = \frac{q_i D_i(x)}{k_b T} E(x) n_i(x) = D_i(x) n_i(x) \frac{q_i}{k_b T} \frac{\partial V(x)}{\partial x}. \quad (4)$$

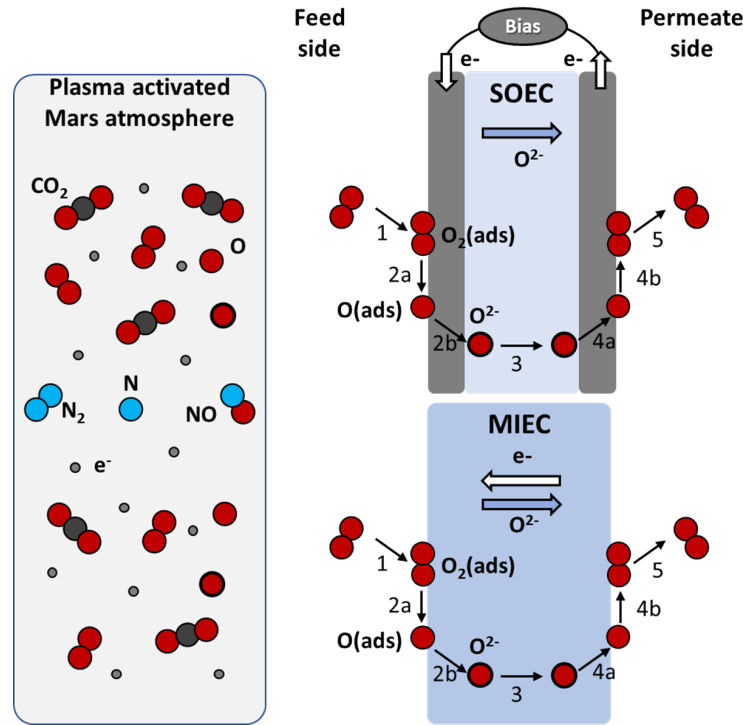


FIG. 2. Schematic representation of oxygen separation via SOEC and MIEC.

In the second equality of (4), μ_i is rewritten as a diffusivity using the Einstein relation, and rearranged in the final equality to have the same form as (2). Note that, for simplicity, changes to the chemical potential of species i are neglected in (4), see Wu and Ghoniem³² for more details. Note that also in this case there can be a concentration-driven term, that leads to the so-called Nernst potential in case the current density is zero.

For an ionic conductor with a constant conductivity for ions of $\sigma_i \propto D_i n_V / T$, the flux through the membrane bulk becomes:

$$\Phi_i = \frac{D_i}{d} n_V \frac{q_i}{k_b T} \Delta V, \quad (5)$$

with n_V the (intrinsic) concentration of vacancies which conducting ions can occupy. The substitution of n_i with n_V follows from the Nernst–Einstein relation, where for every conducting ion i there is a vacancy of opposing charge j with the same diffusivity and $n_V = n_i + n_j$.

For mixed conductor membranes, the expression for the steady-state flux becomes more complicated, due to multiple charged species with different mobilities being set in motion by concentration gradients. Since these species are charged, the local electrostatic potential $V(x)$ depends on the distribution of these species. A limiting case is a mixed conductor with

dominant electronic conductivity and a constant ionic conductivity $\sigma_i \propto D_i n_V / T$, with no external applied voltage.³²

$$\Phi_i = \frac{D_i}{d} n_V \ln \frac{n_i^{\leftarrow}}{n_i^{\rightarrow}}, \quad (6)$$

While Eqs. (3), (5) and (6) are all simplified cases excluding surface reactions, they do convey the general transport behavior: in all cases thinner membranes and increased diffusivity D_i can produce higher fluxes. The latter can be achieved by higher operating temperatures T , since D_i can typically be described by an Arrhenius-type behavior with an exponential factor $e^{-\Delta E/T}$, with ΔE an activation energy. Furthermore, both non-electrochemical and mixed conductors depend on a species gradient as the driving force, while purely ionic conductors depend on an externally applied voltage ΔV .⁸⁶

A. Plasma with non-electrochemical membranes

The best example of a non-electrochemical membrane, designed with Mars ISRU in mind, is represented by the work of Outlaw and co-workers.^{85,92-95} Identifying silver as a membrane with selectivity towards oxygen species, the thermally activated nature of the diffusion coefficient D_O of O atoms in Ag was mapped in the temperature range 673 K – 1073 K,⁸⁵ followed by combination of these membranes with both O₂ and CO₂ glow discharges. For a 320 μm Ag membrane at 923 K, the O₂ flux was improved by a factor of 6.5 when comparing an inert O₂ gas and a 17.5 W O₂ plasma on one side of the membrane.⁹² This improvement is attributed to the rate-limiting step of O₂ needing to stick to Ag, and subsequently dissociating into O atoms prior to transport, being alleviated by the O atom flux from the plasma.

In a follow-up study by Wu *et al* using 350 μm Ag0.05Zr,⁹³ the upstream O atom concentration in the membrane, or n_O^{\leftarrow} in Eq. (3), was determined with and without an O₂ glow discharge, see Figure 3. These data demonstrates that higher throughput can be achieved at lower temperature T with the aid of plasma through an increase in the species gradient. For $T > 800$ K, however, the (sub-)surface O atom concentration (as well as the flux Φ_O) declines to the value without plasma. This is attributed to O atoms rapidly recombining to O₂ and desorbing back into the gas phase at these higher temperatures. Nevertheless, the experiment demonstrates that plasma allows for reduced operating temperatures without

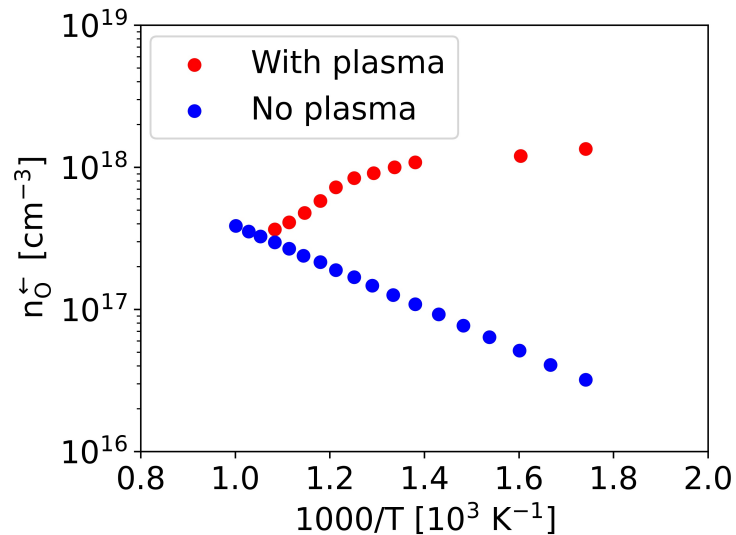


FIG. 3. Sub-surface O atom concentration n_{O}^{\perp} in a Ag membrane, determined from measured O_2 fluxes. Data taken from figure 8 in Wu *et al.*⁹³

sacrificing performance (i.e. the same O_2 flux could be achieved at 570 K compared with 715 K without plasma).⁹³ With the same membrane a similar performance was found for CO_2 plasma and O_2 plasmas.⁹⁴

As Eq. (2) suggests, a clear route towards improved oxygen species transport is using thinner membranes. This was investigated by Premathilake *et al.*, where the previous 350 μm Ag membranes were reduced in thickness to 25 μm .⁹⁵ This 14-fold decrease in thickness was shown to increase O_2 flux from 1×10^{14} molecules/s/cm² to above 1×10^{15} molecules/s/cm² on exposure to a CO_2 glow discharge at the same operating temperature.⁹⁴ While the conditions of the plasmas used in both studies are different in terms of applied power and electrode configuration, most of this improvement can be comfortably assigned to the decrease in membrane thickness.

B. Plasma with mixed conductors

A hollow fiber mixed conductor (Perovskite-type, $\text{La}_{0.6}\text{Ca}_{0.4}\text{Co}_{0.5}\text{Fe}_{0.5}\text{O}_{3-\delta}$, or LCCF: a dominantly electronic conductor) was placed in the effluent of a CO_2 microwave plasma torch by Chen *et al.*³³ The interior of the fiber was continuously flushed by pure Ar, ensuring the highest possible O_2 partial pressure gradient over the 0.2 mm fiber wall. At $T = 1173$ K,

oxygen permeation rates were 1.8×10^{18} molecules/s/cm² in the plasma environment, versus 5.7×10^{17} molecules/s/cm² in an inert gas containing 6.5% O₂. Chen *et al.* also demonstrate that, with a wall thickness of 0.2 mm and without plasma, they operate in a regime where the surface reactions are rate-limiting, i.e. the concentration of oxygen ions achieved in the sub-surface $n_{O_2^-}^{\leftarrow}$ in Eq. 6 reaches a plateau and is not proportional to the partial pressure of O₂ outside the surface. The improved oxygen permeation rates in the plasma environment can, therefore, be attributed to O radicals from the plasma being more readily incorporated into the membrane material than molecular O₂, thus increasing $n_{O_2^-}^{\leftarrow}$ in Eq. 6 compared to the case without plasma.

A mixed conductor (La_{0.6}Sr_{0.4}Co_{0.3}Fe_{0.8}O_{3- δ} , or LSCF, another dominantly electronic conductor) of 1 mm thickness was used as an end cap on a cylindrical DBD by Zheng *et al.*⁹⁶ Operating the DBD at 15 W in air, at $T = 873$ K, improved the oxygen permeation rate by a factor of nearly 30, to 2.8×10^{16} molecules/s/cm². At $T = 1173$ K, however, the oxygen permeation rate was only slightly increased by plasma, to a maximum of 1.2×10^{17} molecules/s/cm². Using data obtained at multiple temperatures, the apparent activation energy for oxygen permeation was shown to decrease from 1.42 eV/molecule to 0.45 eV/molecule. Since bulk diffusivities $D_{O_2^-}$ are unlikely to be affected by plasma species, this improvement can also be attributed to the easier incorporation of oxygen species from the plasma, such as O²⁻, in the membrane.

C. Plasma with oxygen ionic conductor systems

In an experiment by Mori & Tun,⁸⁴ a DBD was operated on top of a Solid Oxide Electrolysis Cell (SOEC) using YSZ as electrolyte. The exterior electrode of the SOEC acted as the ground electrode for the DBD, and power was supplied to the devices separately. The entire assembly was placed inside an oven to allow the YSZ to reach a high enough temperature (> 700 K) to allow for significant oxygen ion conduction at $\Delta V = 5$ V - 10 V across the cell. Using this hybrid system, it was demonstrated that CO₂ conversion could be increased from a maximum of 40% without SOEC to $> 90\%$ with the SOEC under power. The power input to the DBD was 40 W for this case, while the SOEC consumption was below 1 W. It was also shown, however, that the residence time required to achieve maximum conversion increased significantly in hybrid operation. The data indicated that *in operandi* extraction

of oxygen species from the plasma region almost fully negates recombination reactions between CO and O, but CO₂ dissociation reactions are similarly slowed down. It is suggested by Mori and Tun that the reaction



is suppressed due to the effective removal of O atoms from the plasma volume. This work clearly demonstrates the synergistic effects between a hybrid CO₂ plasma/electrolyzer system while simultaneously emphasizing the need for detailed mechanistic studies to assess its full potential.

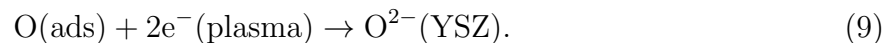
An even more intriguing possibility for merging plasma with electrolysis is to place both devices into a single series circuit and powering both using the same voltage source. In this scheme, one of the electrodes can be moved away from the electrolyzer membrane, creating a gas gap in which a plasma can be ignited. This configuration was investigated by Steinmüller *et al* using pure O₂ DC discharges.⁹⁷ Plasma was successfully ignited in both a Pt|YSZ|plasma|Pt and Pt|YSZ|plasma|YSZ|Pt configuration and compared against a Pt|plasma|Pt baseline. At $T = 820$ K and applied voltage of 1.2 kV, respective currents of 4.7 mA, 6.0 mA and 5.7 mA were observed. With membrane(s) and plasma forming a series circuit, these currents were carried by O²⁻ moving through the YSZ, which clearly does not form a severe limiting factor in sustaining the plasma. Furthermore, only a minor degradation of the 1 mm thick YSZ membranes was evident at temperatures above 570 K, for both polycrystalline and (100) single crystal YSZ, after 20h of operation. Unfortunately, in the experiments of Steinmüller *et al*, the single-sided Pt|YSZ|plasma|Pt configuration was tested only with the YSZ on the anode side of the plasma, meaning that O₂ was supplied to the plasma volume and not extracted. But since their highest currents are achieved in the experiment with YSZ on both sides of the plasma, the extraction of (charged) oxygen species from the cathode side of the plasma is likely the least rate-limiting.

In a conventional SOEC, platina is an effective catalyst for the reaction:



which, depending on oxygen partial pressure, voltage applied on the SOEC, and the microstructural properties of the gas/Pt/YSZ interface, can be a limiting factor in the currents that can be achieved in the cell. With plasma operating in O₂ or CO₂, large fluxes of atomic

O and electrons will impinge on the YSZ surface and allow for a more direct formation of O^{2-} ,⁹¹



Notice that current studies are not about finding the best catalyst, but rather to demonstrate a concept. As Pt is a well known catalyst to convert CO and O_2 into CO_2 , future systems may use different catalysts, or no catalysts at all (see below). To use heated membrane surfaces for oxygen separation remains a challenge, as discussed by Pandiyan *et al.*⁹⁸ Nevertheless, the advantages in terms of improving SOEC material stability in comparison with the same process in the absence of plasma are already established.⁹⁸

Similar to reaction 9, fluxes of negative ions O^- and O_2^- , as well as electronically excited species $O(^1D)$, $O(^1S)$, $O_2(a)$ and $O_2(b)$, could undergo reaction to O^{2-} on the plasma/YSZ interface at potentially higher rates than reaction 8, due to the energy already imparted to these species by the plasma. If reactions like 9 are indeed effective substitutes for 8, as the experiments of Steinmüller *et al* suggest, in parallel with similar observations for non-electrochemical and mixed conductor membranes combined with plasma,^{33,92,93} two advantages of a hybrid plasma/SOEC approach emerge:

- (i) the electrolyzer no longer requires a potentially costly, and prone to degrading, catalytic electrode on its anode side (plasma cathode side);
- (ii) with the plasma supplying energetic species to the YSZ surface, the membrane could become effective at lower operating temperatures.

Point (ii) implicitly assumes that reaction 8 is rate-limiting, which will only be the case for very thin solid oxide membranes in which the bulk impedance to O^{2-} transport is sufficiently low. In the previous sections, effective operation at lower T with the aid of plasma was already shown for Ag membranes,^{92,93} while the rate-limiting nature of O^{2-} incorporation was revealed for 0.2 mm thick mixed conductor membranes.³³

The advantage of ionic conductors compared with non-electrochemical or mixed conductor membranes is the free parameter ΔV (see Eq. (5) compared with Eqs. (3) and (6)): the O_2 flux can be controlled via the applied voltage and does not directly depend on the O_2 concentrations on either side of the membrane. Essentially, an ionic conductor membrane like YSZ can act as a pump for selective transport of O_2 . For Mars ISRU applications, this

Type	Membrane	d [μm]	T [K]	ϕ_{noplasma}^*	$\phi_{\text{O}_2\text{plasma}}$	$\phi_{\text{CO}_2\text{plasma}}$	p [mbar]	Ref.
Non-electrochemical	Ag	320	1173	4.40×10^{13}	2.83×10^{14}	1.74×10^{14}	0.7	85
	Ag0.05Zr	320	723	3.40×10^{12}	2.10×10^{13}	-	4.0	93
	Ag	350	723	1.90×10^{12}	0.60×10^{14}	1.0×10^{14}	6.7	94
	Ag	25	723	-	-	1.61×10^{15}	6.7	95
Mixed conductors	LCCF	200	1173	5.74×10^{17}	-	1.77×10^{18}	1000	33
	LCSF	1000	873	9.9×10^{14}	$2.8 \times 10^{16*}$	-	1000	96
		1173	9.9×10^{16}	$1.2 \times 10^{17*}$	-	1000	96	
Ionic conductors	YSZ (-)	1000	820	-	-	1.27×10^{15}	0.5	97
	YSZ (+&-)	1000	820	-	-	1.33×10^{15}	0.5	
MOXIE	ScSZ	?	1100	2.38×10^{17}	-	-	1000	22

TABLE I. O_2 fluxes [molecules/s/cm²] achieved with various membrane types, with and without plasma. MOXIE is included for comparison, although ScSZ membrane thickness is proprietary knowledge and remains unpublished. The - and + signs identify the anode and the cathode, respectively, while ScSZ stands for “scandia-stabilized zirconia.” The results marked with * were obtained in an air mixture.

could be a distinct advantage since it alleviates the need for separate hardware to minimize the concentration of O_2 on the downstream side of the membrane, as is the case for non-electrochemical or mixed conductor membranes. However, this gain comes with an added complexity of the design.

Table I summarizes the experimental values of O_2 fluxes achieved with different types of membranes. It is worth noting that all these membranes rely on high temperatures to operate. Heating can potentially be supplied by the plasma or alleviated by the plasma effects, which is one of the interesting aspects of merging plasma and membrane technologies.

IV. PLASMA CHEMISTRY

An accurate description of plasma discharges sustained under a Martian environment calls for the detailed understanding of different kinetics (vibrational, chemical, electronic, etc.) involving the species that compose the atmosphere of Mars, including CO_2 , N_2 and Ar, along

with the decomposition products created in the reactor. The development and experimental validation of self-consistent models constitute a powerful tool to obtain insight into the coupled kinetics in these plasmas and to access quantities that are difficult to measure experimentally. The next sub-sections review the current status of plasma chemistry models focusing CO_2 decomposition and NO_x production, respectively. Recent developments and new results are presented as well.

A. CO_2 conversion

In the past few years, several works have been conducted addressing the kinetics of CO_2 and its mixtures with N_2 and/or Ar, as a result of the increasing interest on Mars entry problems.^{99–102} This is a critical research topic for the understanding of heat generation on the surface of spacecrafts and gas dynamic parameters of space vehicles during atmospheric entry. CO_2 plasma discharges produced in the laboratory and sustained under pressures close to the Martian atmosphere, as well as close to Earth's atmospheric pressure, have also been modeled in recent works in the framework of investigations dedicated to solar fuel production and reforming of CO_2 . In particular, the potential of plasmas to induce ladder-climbing mechanisms and molecular dissociation³⁶ has motivated the investigation of the impact of vibrational excitation on CO_2 dissociation. Kozak and Bogaerts^{41,103} have contributed to advance the topic through the development of a zero-dimensional kinetic model of CO_2 splitting with 25 vibrational levels up to the dissociation limit of the molecule, while considering state-specific vibrational-translational (V-T) and vibrational-vibrational (V-V) relaxation reactions and the effect of vibrational excitation on chemical reactions. Additional contributions to this model were made by Pietanza and co-workers, paying particular attention to the self-consistent coupling between the electron energy distribution function (EEDF) and the vibrational distribution function (VDF).^{46,104–106}

In a complementary line of research, joint computational simulations and plasma diagnostics have contributed to a better understanding of the fundamental properties of CO_2 -containing discharges. A combination of modeling tools with experimental campaigns undertaken in DC glow discharges was used to study the relaxation of CO_2 vibrationally excited levels,¹⁰⁷ understand the transfer of electron energy towards CO_2 vibrations,⁵² analyze the influence of N_2 on the CO_2 dissociation yield and vibrational distribution functions,¹⁰⁸ vali-

date the electron-impact dissociation cross sections of CO_2 ,³⁹ investigate the gas heating in the afterglow of pulsed CO_2 discharges,¹⁰⁹ elucidate the role of CO(a) electronically excited metastable states in CO_2 dissociation and CO recombination,^{58,110} and define a reaction mechanism for the formation of CO_2 dissociation products in vibrationally cold plasmas.⁴⁸ Detailed information about these works can be found in Pietanza *et al.*,³⁷ where a synthesis of the current state of knowledge on the physical chemistry of CO_2 plasmas is provided. It is still worth noting that a macroscopic approximate approach for evaluation of the discharge parameters and conversion fraction was presented very recently by Naidis and Babaeva.^{40,111}

A modeling study of discharges produced in the laboratory exclusively dedicated to the Martian environment and ISRU applications was presented recently (see section I).⁴⁷ The role of CO_2 vibrations is revealed, by demonstrating that the cold temperatures of Mars can preserve the asymmetric vibrations of CO_2 , which accumulate energy for the decomposition of CO_2 and subsequent oxygen production. An accompanying experimental campaign characterized DC glow discharges in which the gas was cooled down to Martian temperatures by inserting a plasma reactor inside a cold bath of dry ice and ethanol, both in pure CO_2 and in a synthetic Martian atmosphere (in terms of composition, *i.e.*, including the minor components N_2 and Ar).⁴⁹ Despite the limitations of DC glow discharges in terms of energy efficiency for CO_2 conversion, these plasmas constitute ideal systems for fundamental studies given their simple geometry and the homogeneity of its positive column. These allow the study of CO_2 plasmas using volume average 0D self-consistent kinetic models accounting in detail for the very complex plasma chemistry, as the one developed by Ogloblina *et al.*⁴⁹ It describes the kinetics of electrons and heavy species in DC glow discharges sustained under Martian environment in terms of pressure and temperature, relying on the LisOn KInetics (LoKI) simulation tool¹¹² to solve the homogeneous two-term Electron Boltzmann equation and the system of zero-dimensional (0D, volume averaged) rate balance equations for the most relevant charged and neutral species of a pure CO_2 plasma. The simulation results were in very good agreement with the experimental data and showed that the pressure and temperature conditions of Mars can enhance the degree of vibrational non-equilibrium. Furthermore, the experiments have shown that the Martian atmospheric composition (the minor components N_2 and Ar) has a positive effect on CO_2 decomposition.

Here, we improve the model of Ogloblina *et al.*⁴⁹ by including the: (i) vibrational exchanges between N_2 and CO ,^{113,114} (ii) quenching of CO and CO_2 vibrations by oxygen

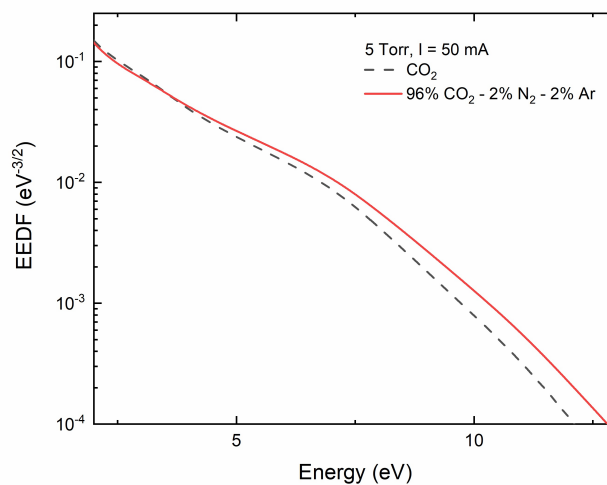


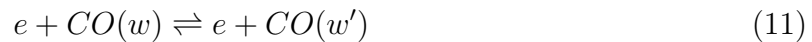
FIG. 4. Electron energy distribution functions calculated for DC glow discharges at $p = 5$ Torr and $I = 50$ mA, for pure CO_2 and for a $96\%\text{CO}_2/2\%\text{Ar}/2\%\text{N}_2$ mixture. The simulations assume a gas temperature of 550 K.⁴⁹

atoms,^{115,116} (iv) V-V and V-T exchanges involving CO molecules,¹¹⁷ (v) vibrational exchanges between CO and CO_2 ,⁹⁹ and (vi) several electron impact, vibrational energy exchanges and reactions involving N_2 ¹¹⁸ and Ar.¹¹⁹

Figure 4 shows the simulated EEDF for a DC glow discharge operated under a continuous regime at a pressure $p = 5$ Torr and a discharge current $I = 50$ mA, both for pure CO_2 and $96\%\text{CO}_2/2\%\text{Ar}/2\%\text{N}_2$ (synthetic Martian mixture). In both cases we consider a gas temperature of 550 K based on the experimental values.⁴⁹ The EEDFs reveal an enhancement of the tail of the EEDF for the Martian mixture in the region of energies above 5 eV (as it was also observed before⁴⁹), related to the differences in the cross sections of the different gases considered in the model and the associated changes in the self-consistent sustaining reduced electric field (that increases from 59 Td in pure CO_2 to 67 Td in the Martian $\text{CO}_2/\text{Ar}/\text{N}_2$ mixture). As the threshold for electron impact dissociation is above 6 eV¹²⁰, the effect justifies the observed enhanced dissociation in a Martian atmosphere in comparison with a pure CO_2 discharge.

The electron and heavy-particle kinetics are strongly coupled due, to a big extent, to the modifications of the EEDF as result of inelastic and superelastic collisions with vibrationally

excited molecules,^{49,104,121}



where ν and ν' denote generic CO_2 vibrational levels in the form $v \equiv (\nu_1\nu_2^{l_2}\nu_3)$, ν_1 , ν_2 and ν_3 are the vibrational quanta associated with the symmetric stretch, bending and asymmetric stretch vibration modes, l_2 defines the projection of the angular momentum of bending vibrations onto the axis of the molecule,¹⁰⁷, w and w' are vibrational levels of CO, and v and v' are vibrational levels of N_2 . Considering that the EEDF is central to estimate the CO_2 conversion, the description of the vibrational distributions and vibrational temperatures associated with the molecules that compose the Martian plasmas is of special importance. The calculated vibrational distributions of N_2 , CO, CO_2 asymmetric levels and CO_2 bending levels are shown in figure 5, for the same conditions as in figure 4. The corresponding “vibrational temperatures,” T_{N_2} , T_{CO} , T_3 and T_{12} , are given in table II, together with the experimental data obtained for the same conditions. Note that the vibrational temperatures are calculated by fitting the very first points of the vibrational distributions to a Boltzmann distribution. There is a generally good agreement between the predicted and measured vibrational temperatures. More striking, the simulations evince a remarkable deviation from equilibrium for N_2 and CO, emphasizing the importance of detailed state-to-state models and of an understanding of the vibrational energy transfers taking place in the system.

Parameter	Experiment	Model
T_{12} (K)	600	612
T_3 (K)	800	956
T_{CO} (K)	800	1063
T_{N_2} (K)	-	1031
N_e (m^{-3})	-	9.8×10^{15}

TABLE II. Measured and calculated values associated to vibrational temperatures and electron density (N_e) in a DC glow discharge operating at $p = 5$ Torr and $I = 50$ mA, for a 96% CO_2 /2%Ar/2% N_2 gas mixture. The simulations assume a gas temperature of 550 K.⁴⁹

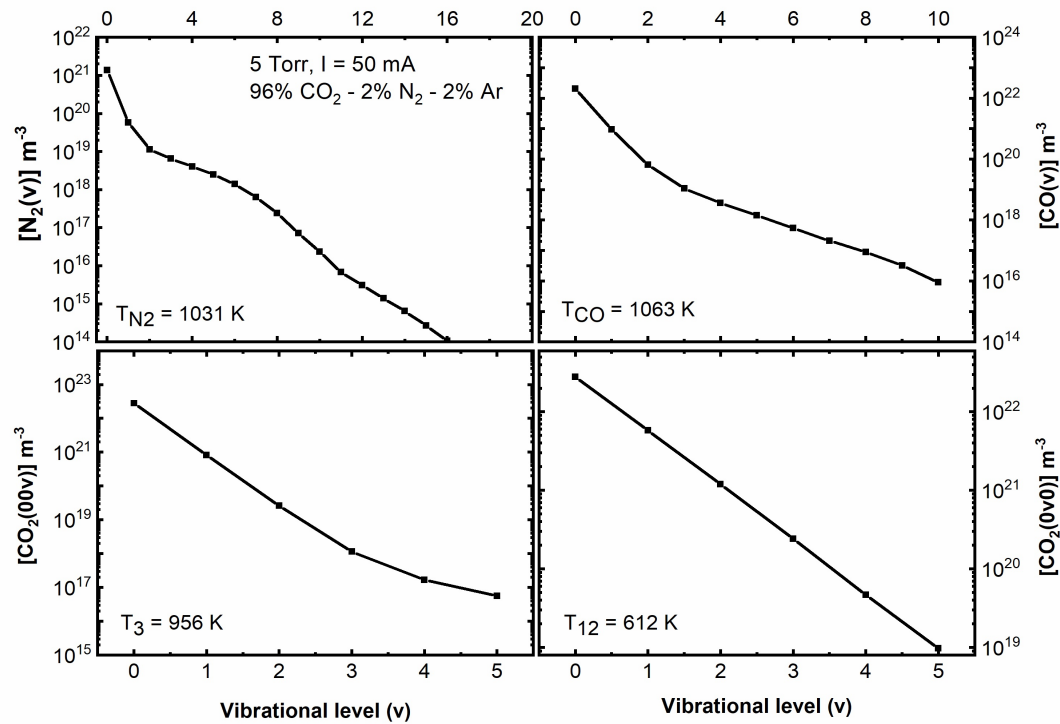
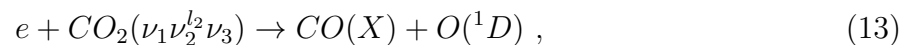
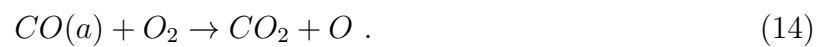


FIG. 5. Vibrational distribution functions of N_2 , CO , asymmetric stretch mode of CO_2 and bending mode of CO_2 , calculated for a DC glow discharge operating at $p = 5$ Torr and $I = 50$ mA, for a 96% CO_2 /2% Ar /2% N_2 gas mixture. The simulations assume a gas temperature of 550 K.⁴⁹

In the present conditions, CO_2 dissociation proceeds mainly by direct electron impact on CO_2 ground-state and vibrationally excited molecules,⁴⁹



where the levels (00^0_0) , (01^1_0) , (02^2_0) , and $(10^0_0 + 02^0_0)$ have the most important contributions. In continuous operation, electronically excited $CO(a)$ molecules promote CO recombination into CO_2 , due to bimolecular reactions as^{58,110}



Nonetheless, it has been noted that for small O_2 concentrations CO_2 dissociation can be stimulated through



attesting the complex role this electronically excited state can play in the overall kinetics.

For completeness, the calculated concentrations of the dominant neutral species formed in the plasma are given in table III. Along with the main CO₂ decomposition products (CO and oxygen species) we observe the creation of other interesting products in the context of ISRU on Mars, namely NO and NO₂, which are further discussed in the next sub-section.

Species	Concentration (m ⁻³)
CO ₂ (X)	4.88×10^{22}
N ₂ (X)	1.45×10^{21}
Ar(¹ S ₀)	1.47×10^{21}
Ar(4s)	3.29×10^{11}
CO(X)	2.16×10^{22}
CO(a)	2.98×10^{16}
O ₂ (X)	6.73×10^{21}
O ₂ (a)	4.37×10^{20}
O ₂ (b)	7.69×10^{17}
O(³ P)	7.29×10^{21}
O(¹ D)	2.63×10^{16}
O ₃ (X)	8.62×10^{16}
NO(X)	3.13×10^{19}
NO ₂ (X)	8.09×10^{14}

TABLE III. Calculated concentrations for the main species in the plasma in a DC glow discharge operating at $p = 5$ Torr and $I = 50$ mA, for a 96%CO₂/2%Ar/2%N₂ gas mixture. The simulations assume a gas temperature of 550 K.⁴⁹

It is worth highlighting that, despite their relatively small concentration, electronically excited states play a relevant role in the overall kinetics,^{48,49,60} as exemplified above for the case of CO(a). Together with vibrationally excited states they can be important energy carriers and, depending on the operating conditions and discharge type, may participate in dissociation, recombination and gas heating.

The DC discharges studied here are very useful for validation of kinetic schemes and gaining insight into the elementary processes taking place in the plasma. Future studies will

need to consider other plasma sources and verify the applicability of these models to the higher E/N regimes and fast-pulsed discharges. A thorough analysis and further validation of the results presented here will be addressed in a future publication.

B. NO production

One advantage of using plasma sources for *in situ* resource utilization is their versatility to synthesize different compounds. Indeed, by using different gases to produce various molecules of interest, the same power sources and principles outlined for CO_2 decomposition can be adapted for other gas-conversion applications. For instance, exposing the transported O to activated N_2 leads to the formation of NO_x , essential for the synthesis of fertilizers and nitrogen fixation. These processes are being pursued for agriculture and the food industry on Earth,^{122–124} and an adaptation using N_2 from the Martian atmosphere (and O extracted from CO_2) can be envisioned on Mars.

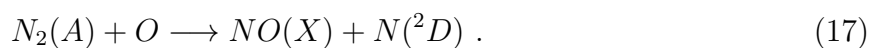
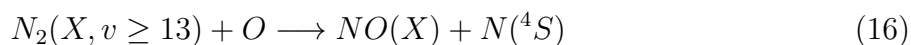
On Earth, nitrogen fertilizers are very often synthesized from ammonia (NH_3) and aim to provide plants with the ammonium ion (NH_4^+). If a sufficient source of hydrogen is available on Mars, ammonia can be synthesized with non-thermal plasmas. Gas phase plasma chemistry induced by electrons is of great importance,^{122–124} but plasma-surface interactions should also be accounted for. For example, it was shown that in RF plasmas of N_2/H_2 at a few mbar NH_3 is produced mostly on surfaces in direct contact with the plasma.^{125–127} However, many crops incorporate nitrate (NO_3 anion) even faster than NH_4^+ .¹²⁸ Producing nitrate on Mars first requires the production of NO_x from atmospheric nitrogen and oxygen produced from CO_2 dissociation, and is the focus of the present sub-section.

On Earth, plasmas ignited in air are known to produce significant quantities of NO and NO_2 . The optimisation of NO_x production efficiency by plasma has been widely studied at atmospheric pressure. Energy efficiencies of the order of 5 MJ/mol of NO have been obtained with spark, gliding arc or microwave plasma sources.^{129,130} These plasmas have a large energy deposition and induce high gas temperatures at atmospheric pressure. Nevertheless, NO_x production is also achievable at low pressure (albeit with lower energy efficiencies *e.g.* 0.8 MJ/mol at 60 Torr in a MW discharge¹³¹) by taking advantage of the non-equilibrium character of non thermal plasmas.

The kinetics of air plasmas has been studied for a long time for various applications such

as ozone production,^{132,133} indoor air pollution control,^{134–136} surface sterilization,^{137,138} or atmospheric re-entry shields.^{139,140} The mechanisms of NO_x formation in cold plasmas at reduced pressure are therefore relatively well known and have been described in various modeling works.^{141–144} A recent review article compiles the latest results on the description of the plasma kinetics of N_2/O_2 , including the formation of NO_x .¹¹⁸

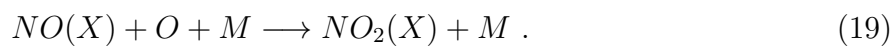
In N_2/O_2 plasmas NO is mainly formed in collisions of O atoms with vibrationally excited $\text{N}_2(X^1\Sigma_g^+, v \geq 13)$ or metastable states $\text{N}_2(A^3\Sigma_u^+)$,^{145,146}



The vibrational distribution of N_2 in non-thermal plasmas at few mbar can often be described by a Treanor distribution accounting for an overpopulation of intermediate and high vibrational states.¹⁴⁷ Nevertheless, reaction (16) is so efficient that it can induce a strong depletion of $v \geq 13$ states.^{148,149} Other NO formation processes from collisions between N atoms and O_2 atoms exist but are usually much less efficient, partly because of the lower density of N atoms compared with O (typically the N atomic density is ≈ 10 times lower than that of O). On the other hand, nitrogen atoms play an important role in the destruction of NO , by reaction^{145,148}



NO_2 is mainly formed by a 3-body reaction in collisions of NO with oxygen atoms,¹⁴⁶



The NO_x formation increases significantly with pressure in the range of 1 to 10 mbar.¹⁴⁴ All these processes result in a maximum of NO formation for N_2/O_2 mixtures containing 40 to 50% O_2 .^{142,144,150} Therefore, an optimum NO_x production on Mars by plasma can be obtained using directly the O_2 produced at a few mbar at the outlet of a CO_2 conversion reactor, and adding to it an equal proportion of N_2 previously separated from the $\sim 2\%$ of N_2 present in Martian atmosphere.

Reactions (16) to (19) concern creation/loss processes in the gas phase, but it is evident that surfaces play an important role in the kinetics of NO_x in plasmas at a few mbar. As a matter of fact, at these low pressures the recombination of O and N atoms is mainly

controlled by recombination at the walls,¹⁴⁵ and these atomic species are directly involved in reactions (16) to (19). The probability of recombination of the atoms (noted γ_O or γ_N , respectively for O and N) depends on the material, its roughness, the surface temperature and whether or not the surface is directly exposed to the plasma, among other things. Typical values of γ_O and γ_N can vary from 10^{-4} to 10^{-2} .¹⁵¹

NO and NO₂ can also be formed on surfaces.^{142,152–154} The strong interdependence between surface and gas phase kinetics on the proportion of NO_x produced in the gas phase has already been investigated by modelling.^{142,143} However, the high variability of γ values and the lack of experimental data on the surface reactivity for different materials still demands for significant research efforts in order to allow accurate predictions of the influence of surfaces on NO_x production. Nevertheless, the possibility of forming NO and of converting NO to NO₂ from oxygen atoms adsorbed on a surface even as inert as glass (SiO₂) was evidenced experimentally with DC glow discharges, microwave post-discharges or downstream arc discharges.^{155–157} The oxidation of NO into NO₂ with adsorbed O atoms, following the reaction (19) with the wall playing the role of the third body, could even be used as a test case to demonstrate the existence of a continuous distribution of adsorption energies of O atoms on Pyrex by comparing modeling and experimental results.¹⁵⁴ Therefore, a suitably engineered surface placed either in direct contact with the plasma or in a post-discharge, for instance from a microwave source, could improve the NO_x production efficiency. In turn, an increase in NO/NO₂ production efficiencies due to the presence of a MoO₃ catalyst downstream of a microwave discharge was observed in early works on the subject,¹³¹ suggesting plasma-catalysis as another route to explore.

The production of NO_x on surfaces under direct plasma exposure can also benefit from the coupling with an ion conducting membrane, as discussed for CO₂ conversion in section III. Indeed, a pure N₂ plasma can be generated on one side of the membrane, while an oxygen flow resulting from the conversion of CO₂ on the other side can diffuse through the membrane. The atomic oxygen adsorbed on the surface can then react with excited nitrogen species to form NO directly at the surface. This concept was already demonstrated with a YSZ membrane, but the oxygen was produced by water electrolysis instead of CO₂ dissociation.¹⁵⁸ The production of NO obtained was more than 3 orders of magnitude higher than the equilibrium concentration of NO for the same gas mixture and temperature conditions.¹⁵⁸ It is not clear whether the NO formation at the membrane surface was due to N atoms or

to vibrationally excited N_2 molecules, but in any case NO was only produced at the surface when the N_2 plasma was ignited. In any case, the plasma-membrane approach can have several advantages: (i) by igniting the plasma in pure N_2 , the vibrational excitation of the molecules is maximized by limiting the quenching of the vibrational states by oxygen species; (ii) the oxygen required for NO formation can be optimally tuned by playing on the voltage and temperature controlling the oxygen flow through the membrane in order not to waste oxygen previously produced by CO_2 dissociation.

V. FIGURES OF MERIT

This section carries out an estimation of the performance attainable by a plasma-YSZ reactor for O_2 production from the Martian atmosphere, and establishes its high potential from the comparison with MOXIE. Clearly, a proof-of-principle reactor should meet the performance targets defined by MOXIE. In particular, it should:

- operate with a power supply of 300 W or lower;
- operate directly in a synthetic Martian atmospheric gas mixture (96% CO_2 /2% N_2 /2%Ar);
- have reduced dimensions, below $24 \times 24 \times 31 \text{ cm}^3$;
- have reduced weight, below 15 kg;
- produce and separate O_2 , at a rate above 5.5 g per hour.

As discussed in section II, the energy efficiency for plasma conversion of CO_2 varies depending on the plasma source and attained CO_2 conversion, with the highest energy efficiencies observed at low CO_2 conversion, and vice-versa. Typical values for MW and RF discharges, corresponding to a trade-off between energy efficiency and conversion, are around 45% energy efficiency at 30% CO_2 dissociation.^{37,38,45} Preliminary results in MW discharges operating at a power of 300 W in the synthetic Martian atmosphere mixture attained 35% CO_2 dissociation,⁵⁰ compatible with the literature in pure CO_2 . Herein we focus our analysis assuming a (conservative) O_2 production of 14 g per hour.⁴⁹

Regarding separation (see section III), considering an YSZ ion conductivity of $\sim 1 \text{ S/m}$, YSZ thickness $\sim 1 \text{ mm}$, a cylindrical configuration with radius $\sim 1 \text{ cm}$, and a voltage

of 2 V (~ 100 W), the tube length required to reach the target 14 g/O₂ per hour would be ~ 35 cm. Assuming that all the O/O₂ created from the plasma is extracted through such a tubular membrane, the energy efficiency required to produce the necessary O-atom concentrations with a plasma source operating at 200 W (to be added with the power used at the YSZ cell, for a total of 300 W), is around 20-25%, well within reach of current plasma technologies.^{37,38} How effective can a plasma-membrane system extract the oxygen is an open and critical research question.

The numbers above lead to a specific energy of $300 \times 3600/14 \sim 80$ kJ/g of produced O₂ (or, equivalently, ~ 800 kJ/m³, at $p \simeq 4.5$ Torr and $T = 250$ K). This is the first figure of merit to be compared with ~ 195 kJ/g from the current production in MOXIE (or with the results of any other technologies having the same objective).

The target of 6 kg for the reactor is estimated from an optimised reactor, adding up to ~ 3 kg (see the last paragraph of Ogloblina *et al*⁴⁹ for a detailed analysis of this value), estimated for a solid-state MW reactor. A safety factor of 2 is considered to correct for the need of unforeseen elements or additional weight imposed by the optimised design configuration.

This analysis and the preliminary results already obtained allow to estimate that oxygen can be produced at the rate of 14 g/h using a 6 kg reactor with dimensions $25 \times 20 \times 5$ cm³ (including main components and shielding),^{49,50} amounting to 2.33 g of oxygen produced per hour per kg of equipment sent to Mars. These values are the additional figures of merit to be compared with MOXIE's 5.5 g/h at 300 W for a 15 kg reactor of $24 \times 24 \times 31$ cm³, corresponding to 0.37 g of oxygen produced per hour per kg. Accordingly, a plasma based technology can potentially outperform the current state-of-the-art technology defined by MOXIE.

It is still worth noting that the reliability of the plasma sources that can be used in a prototype have been proved in industry already for decades, by their use in microelectronics¹⁵⁹ and Hall-effect thrusters for space propulsion.^{160,161} These sources have a long lifetime, essentially limited by the lifetime of the power supply itself, estimated to be larger than 100,000 hours. For MW and certain RF configurations⁵⁸ there is no contact between electrodes and the plasma, which prevents erosion and increases durability. Finally, the electromagnetic noise emitted by the sources can impose some constraints to the design of the system, but, if required, the system can be shielded with a simple and light grid to act as Faraday cage.

Additional hardware requirements will be needed for a flight qualification plan for a full-

scale mission to Mars. Their realistic assessment can only be done after the demonstration of the integration of the technologies at higher TRL levels. In any case, ground testing should address durability, heat integration for smooth start and stop of the process, and submission of the prototype to relevant mechanical (compression, vibration, shock), thermal and radiation environments to survive launching, space travel, landing and onsite operation.²⁵ Another aspect to consider is the dust presence in the Martian atmosphere and how to filter and clean the system. A full scale system should be able to produce 100 times more O₂ than anticipated by MOXIE.^{22,25} This estimation is compatible with the requirement for a production rate of about 50 kg/day \simeq 2 kg/hr of a propellant manufacturing system for a Mars Ascent Vehicle (MAV).^{16,2} Scalability studies should analyze oxygen production capacity, mass and volume, power requirements, and scaling of specific components. By the very nature of plasma technologies, scalability is not expected to become a major point of concern.

VI. CONCLUSIONS AND OUTLOOK

In-Situ Resource Utilization (ISRU) is the use of natural resources from the Moon, Mars, and other bodies for use in-situ or elsewhere in the Solar System. The most useful mission consumable products from ISRU are propellants, fuel cell reactants, and life support commodities (such as water, oxygen, and buffer gases). Making oxygen alone can provide significant mission savings, as it can be used for these purposes and also for the development of fertilizers for agriculture.¹⁶

This paper opens the perspective of combining non-thermal plasmas with conducting membranes to produce oxygen by decomposing CO₂ directly from the Martian atmosphere and separate the products of CO₂ dissociation, respectively. The current state of the art regarding O₂ production on Mars is defined by MOXIE,²¹⁻²⁵ which is based on solid electrolysis cells (SOEC), where electricity is provided between two electrodes to electrochemically convert CO₂ into oxygen at temperatures above 1000 K and pressures of about 1 bar. MOXIE is a thrilling project and already operates on Mars. Nonetheless, the need to compress and heat the system increases the weight and power consumption of the system, and the erosion of the electrodes is a point of concern.

The approach suggested here brings a solution for ISRU on Mars that can be seen as an

upgraded system when compared with MOXIE. Plasmas can enable activation of CO_2 and thus enhance the performance of the SOEC electrode material towards an efficient oxygen separation, and can be readily ignited at Martian ambient pressure.^{47,49} The combination of plasma with oxygen separation membrane based systems holds the promise of a high performance, both in terms of the required specific energy (energy spent per kg of produced O_2) and of the quantity of oxygen molecules produced per kg of instrumentation placed on Mars. It is very versatile, due to its adaptability to work with different feed-stock and tuneable reactivity depending on the desired outcome. As examples, if H_2 is carried from Earth or produced from electrolysis on Mars, the same reactor used to produce oxygen and CO can be operated in a $\text{CO}_2\text{-H}_2$ mixture to produce methane, that can be used directly as a fuel, in a $\text{N}_2\text{-O}_2$ mixture to produce NO_x , or in a $\text{N}_2\text{-H}_2$ mixture to produce NH_3 ,¹⁶³ the latter two of direct use for Martian agriculture. Additionally, a plasma system can fully decompose CO_2 up to carbon, of interest for the manufacture of carbon structures.

Different plasma sources promote CO_2 dissociation according to alternative concepts. For instance, in radio-frequency (RF) discharges, the CO_2 vibrational kinetics is expected to have a relevant contribution, as the typical mean electron energy (~ 1 eV) favours vibrational excitation; in nanosecond repetitively pulsed (NRP) discharges, the high electric field increases the number of enough-energetic electrons able to directly dissociate CO_2 , offering an alternative route to dissociation that does not rely on vibrational excitation; microwave (MW) discharges operate in yet another regime, where thermal dissociation plays a significant role.

The coupling of plasma with conducting membranes for product separation is an active field of research. Mixed electron-ion conducting (MIEC) membranes^{32-34,64} and ion-conducting membranes^{30,31,158} to be integrated in a plasma reactor are currently under development. The usage of plasma with a conducting membrane may not require the expensive, complex and sensitive cathode materials needed to split oxygen molecules in a conventional solid oxide electrolyzer cell (SOEC). It should enhance the oxygen permeation through the membrane, for two reasons: the prior dissociation of CO_2 in the plasma, and the heat produced by the plasma. On the one hand, plasma dissociation will significantly increase the density of O atoms on the surface of the membrane; in principle, a 100% dissociation of CO_2 into CO and O_2 is possible, provided a sufficiently high residence time is used.⁸⁴ On the other hand, the ionic conductivity becomes significant above a certain temperature (about

600 K for YSZ); in the plasma-membrane combined setup, the membrane can be heated by the plasma itself without the need for additional pre-heating equipment, with another gain in the mass and power requirements of the system. Additionally, the presence of free electrons from the plasma may increase the surface kinetics and contribute as well to an increase of the permeation fluxes.³³

A compromise must be found between the efficiency of dissociation in the plasma volume and the oxygen flow through the membrane: on the one hand, a long residence time of the plasma in the reactor benefits the separation process; on the other hand, the presence of O₂ hinders further plasma dissociation. Furthermore, the temperature of the membrane can in principle be regulated through a combination of power and flow in the plasma, where an optimum working point which provides both a sufficient CO₂ dissociation and the desired translation gas temperature for heating should be accessible. A simple system to impose a small gas flow in a reactor operating on Mars may then have to be included to control the gas residence time. Nonetheless, to know how effectively can a plasma-membrane system extract the oxygen is an open and critical research question.

Kinetic schemes describing the plasma chemistry in CO₂, N₂, Ar and their mixtures, are to a large extent already available. Validation in a Martian environment is still scarce,⁴⁹ but those first results and the ones presented here are very encouraging. The simulations reveal the important role of vibrational excitation and of electronically excited states both in shaping the electron energy distribution function and in the very mechanisms of CO₂ dissociation and CO recombination.³⁷ Validated reaction schemes for N₂-O₂ plasmas, of interest for nitrogen fixation and the production of fertilizers, are also available in the literature.^{118,124} Surface kinetics studies are less developed than their gas volume counterparts and should become an important subject of research in the next few years.³⁷ These studies should improve the description of the elementary steps involved in surface adsorption, diffusion and recombination under plasma exposure, as well as of the bulk diffusion through the membrane. Overall, the current degree of sophistication and the predictive power of plasma models hints at their importance in the design and optimization of future prototypes.

The successful association of plasmas with ion-conducting membranes has not been achieved to date, whereas coupling plasmas with MIEC is at its very first steps. Notwithstanding, the emerging plasma-membrane technology and the solutions outlined here are already founding a new active and probably long-lasting field of activity, associated with

the development of a novel and highly versatile electrochemical conversion technology, that can be applied in different environments on Earth and to several ISRU applications.

ACKNOWLEDGEMENTS

This work was partially supported by: the Portuguese FCT-Fundação para a Ciência e a Tecnologia, under projects UIDB/50010/2020, UIDP/50010/2020, MIT-EXPL/ACC/0031/2021 (CREATOR), EXPL/FIS-PLA/0076/2021 (ROADMARS); The Portuguese Foundation for International Cooperation in Science, Technology and Higher Education through the MIT-Portugal Program (project IMPACT); the European Space Agency (ESA) under project I-2021-03399 (PERFORMER).

We are grateful to Benjamin Martell and Ahmed Ghoniem for their insightful comments and fruitful discussions.

REFERENCES

- ¹G. A. Landis, “Colonization of Venus,” AIP Conference Proceedings **654**, 1193–1198 (2003).
- ²T. B. Kerwick, “Colonizing Jupiter’s moons: An assessment of our options and alternatives,” Journal of the Washington Academy of Sciences **98**, 15–26 (2012).
- ³E. Musk, “Making humans a multi-planetary species,” New Space **5**, 46–61 (2017).
- ⁴D. Rapp, *Use of Extraterrestrial Resources for Human Space Missions to Moon or Mars*, 2nd ed. (Springer, 2018).
- ⁵Indian Space Research Organisation (ISRO), “Mars orbiter mission,” <https://www.isro.gov.in/pslv-c25-mars-orbiter-mission> (2013).
- ⁶China National Space Administration (CNSA), “Chang’e 5,” <http://www.cnsa.gov.cn/english/n6465652/n6465653/c6810558/content.html> (2020).
- ⁷Mohammed bin Rashid Space Centre (MBRSC), “Emirates mars mission,” <https://emiratesmarsmission.ae/> (2020).
- ⁸China National Space Administration (CNSA), “Tianwen-1,” <http://www.cnsa.gov.cn/english/n6465652/n6465653/c6812390/content.html> (2020).

- ⁹Japan Aerospace Exploration Agency (JAXA), “Smart lander for investigating moon (slim),” <https://global.jaxa.jp/projects/sas/slim/> (2022).
- ¹⁰Korea Aerospace Research Institute (KARI), “Korea pathfinder lunar orbiter,” https://www.kari.re.kr/eng/sub03_07.do (2022).
- ¹¹European Space Agency (ESA) and Russian State Space Corporation (Roscosmos), “Luna 25 (luna-glob lander),” https://www.esa.int/Science_Exploration/Human_and_Robotic_Exploration (2022).
- ¹²National Aeronautics and Space Administration (NASA), “Psyche,” <https://psyche.asu.edu/> (2022).
- ¹³European Space Agency (ESA) and Russian State Space Corporation (Roscosmos), “Exobiology on mars (exomars),” https://www.esa.int/Science_Exploration/Human_and_Robotic_Exploration (2022).
- ¹⁴Japan Aerospace Exploration Agency (JAXA), “Martian moons exploration,” <https://www.mmx.jaxa.jp/en/> (2024).
- ¹⁵NASA, “The Artemis plan,” <https://www.nasa.gov/specials/artemis/> (2020).
- ¹⁶International Space Exploration Coordination Group, “In-situ resource utilization gap assessment report,” <https://www.globalspaceexploration.org/wordpress/wp-content/uploads/2021/04/ISECG-ISRU-Technology-Gap-Assessment-Report-Apr-2021.pdf> (2021).
- ¹⁷G. A. Landis and D. L. Linne, “Mars Rocket Vehicle Using In Situ Propellants,” *Journal of Spacecraft and Rockets* **38**, 730–735 (2001).
- ¹⁸M. Rashid, Q. Hussain, K. S. Khan, M. I. Alwabel, R. Hayat, M. Akmal, S. S. Ijaz, S. Alvi, and O. ur Rehman, “Carbon-based slow-release fertilizers for efficient nutrient management: Synthesis, applications, and future research needs,” *J. Soil Sci. Plant Nutr.* **21**, 1144–1169 (2021).
- ¹⁹B. M. Hoffman, D. Lukoyanov, Z.-Y. Yang, D. R. Dean, and L. C. Seefeldt, “Mechanism of nitrogen fixation by nitrogenase: The next stage,” *Chem. Rev.* **114**, 4041–4062 (2014), pMID: 24467365, <https://doi.org/10.1021/cr400641x>.
- ²⁰R. M. Candanosa, “Growing green on the red planet,” *ChemMatters* , 5–7 (2017).
- ²¹M. H. Hecht, D. R. Rapp, and J. A. Hoffman, “The Mars Oxygen ISRU experiment (MOXIE),” in *International Workshop on Instrumentation for Planetary Missions* (Greenbelt, MD, 2014) p. 1134.

- ²²D. Rapp, J. A. Hoffman, F. Meyen, and M. H. Hecht, “The mars oxygen ISRU experiment (MOXIE) on the mars 2020 rover,” AIAA SPACE 2015 Conference and Exposition , 1–12 (2015).
- ²³M. H. Hecht and J. A. Hoffman, “The mars oxygen ISRU experiment (MOXIE) on the mars 2020 rover,” in *3rd International Workshop on Instrumentation for Planetary Missions* (Pasadena, CA, 2016) p. 4130.
- ²⁴E. Hinterman and J. A. Hoffman, “Simulating oxygen production on mars for the mars oxygen in-situ resource utilization experiment,” *Acta Atronaut.* **170**, 678–685 (2020).
- ²⁵M. Hecht *et al*, “Mars oxygen ISRU experiment (MOXIE),” *Space Sci. Rev.* **217**, 9 (2021).
- ²⁶National Aeronautics and Space Administration (NASA), “Mars 2020,” <https://mars.nasa.gov/mars2020/> (2020).
- ²⁷Y. Zheng, J. Wang, B. Yu, W. Zhang, J. Chen, J. Qiao, and J. Zhang, “A review of high temperature co-electrolysis of H₂O and CO₂ to produce sustainable fuels using solid oxide electrolysis cells (soecs): advanced materials and technology,” *Chem. Soc. Rev.* **46**, 1427–1463 (2017).
- ²⁸V. Kyriakou, D. Neagu, E. Papaioannou, I. Metcalfe, M. van de Sanden, and M. Tsampas, “Co-electrolysis of H₂O and CO₂ on exsolved Ni nanoparticles for efficient syngas generation at controllable H₂/CO ratios,” *Appl. Catal. B* **258**, 117950 (2019).
- ²⁹A. Hauch, M. Traulsen, R. Küngas, and T. Skaftø, “CO₂ electrolysis - gas impurities and electrode overpotential causing detrimental carbon deposition,” *J. Power Sources* **506**, 230108 (2021).
- ³⁰A. Pandiyan, V. Kyriakou, D. Neagu, S. Welzel, A. Goede, M. C. van de Sanden, and M. N. Tsampas, “CO₂ conversion via coupled plasma-electrolysis process,” *J. CO₂ Util.* **57**, 101904 (2022).
- ³¹V. Kyriakou, R. K. Sharma, D. Neagu, F. Peeters, O. De Luca, P. Rudolf, A. Pandiyan, W. Yu, S. W. Cha, S. Welzel, M. C. van de Sanden, and M. N. Tsampas, “Plasma driven exsolution for nanoscale functionalization of perovskite oxides,” *Small Methods* **5**, e2100868 (2021).
- ³²X. Y. Wu and A. F. Ghoniem, “Mixed ionic-electronic conducting (MIEC) membranes for thermochemical reduction of CO₂: A review,” *Prog. Energy Combust. Sci.* **74**, 1–30 (2019).

- ³³G. Chen, F. Buck, I. Kistner, M. Widenmeyer, T. Schiestel, A. Schulz, M. Walker, and A. Weidenkaff, "A novel plasma-assisted hollow fiber membrane concept for efficiently separating oxygen from CO in a CO₂ plasma," *Chem. Eng. J.* **392**, 123699 (2020).
- ³⁴G. Chen, A. Feldhoff, A. Weidenkaff, C. Li, S. Liu, X. Zhu, J. Sunarso, K. Huang, X.-Y. Wu, A. F. Ghoniem, W. Yang, J. Xue, H. Wang, Z. Shao, J. H. Duffy, K. S. Brinkman, X. Tan, Y. Zhang, H. Jiang, R. Costa, K. A. Friedrich, and R. Kriege, "Roadmap on sustainable mixed ionic-electronic conducting membranes," *Adv. Funct. Mater.* **32**, 2105702 (2022).
- ³⁵Y. P. Raizer, *Gas discharge physics* (Springer-Verlag, 1991).
- ³⁶A. Fridman, *Plasma Chemistry* (Cambridge University Press, 2008).
- ³⁷L. D. Pietanza, O. Guaitella, V. Aquilanti, I. Armenise¹, A. Bogaerts, M. Capitelli, G. Colonna, V. Guerra, R. Engeln, E. Kustova, A. Lombardi, F. Palazzetti, and T. Silva, "Advances in non-equilibrium CO₂ plasma kinetics: a theoretical and experimental review," *Eur. Phys. J. D* **75**, 237 (2021).
- ³⁸A. George, B. Shen, M. Craven, Y. Wang, D. Kang, C. Wu, and X. Tu, "A review of non-thermal plasma technology: A novel solution for CO₂ conversion and utilization," *Renew. Sustain. Energy Rev.* **135**, 109702 (2021).
- ³⁹A. S. Morillo-Candas, T. Silva, B. L. M. Klarenaar, M. Grofulović, V. Guerra, and O. Guaitella, "Electron impact dissociation of CO₂," *Plasma Sources Sci. Technol.* **29**, 01LT01 (2020).
- ⁴⁰N. Y. Babaeva and G. Naidis, "On the efficiency of CO₂ conversion in corona and dielectric-barrier discharges," *Plasma Sources Sci. Technol.* **30**, 03LT03 (2021).
- ⁴¹T. Kozák and A. Bogaerts, "Evaluation of the energy efficiency of CO₂ conversion in microwave discharges using a reaction kinetics model," *Plasma Sources Sci. Technol.* **24**, 015024 (2015).
- ⁴²M. Capitelli, G. Colonna, G. D'Ammando, and L. D. Pietanza, "Self-consistent time dependent vibrational and free electron kinetics for CO₂ dissociation and ionization in cold plasmas," *Plasma Sources Sci. Technol.* **26**, 055009 (2017).
- ⁴³F. A. D'Iza, E. A. D. Carbone, A. Hecimovic, and U. Fantz, "Performance analysis of a 2.45 GHz microwave plasma torch for CO₂ decomposition in gas swirl configuration," *Plasma Sources Sci. Technol.* **29**, 105009 (2020).
- ⁴⁴A. J. Wolf, T. W. H. Righart, F. J. J. Peeters, W. A. Bongers, and M. C. M. van de

- Sanden, “Implications of thermo-chemical instability on the contracted modes in CO₂ microwave plasmas,” *Plasma Sources Sci. Technol.* **29**, 025005 (2020).
- ⁴⁵A. J. Wolf, F. J. J. Peeters, P. W. C. Groen, W. A. Bongers, and M. C. M. van de Sanden, “CO₂ conversion in nonuniform discharges: Disentangling dissociation and recombination mechanisms,” *J. Phys. Chem. C* **124**, 16806 (2020).
- ⁴⁶L. D. Pietanza, G. Colonna, and M. Capitelli, “Self-consistent electron energy distribution functions, vibrational distributions, electronic excited state kinetics in reacting microwave CO₂ plasma: An advanced model,” *Phys. Plasmas* **27**, 023513 (2020).
- ⁴⁷V. Guerra, T. Silva, P. Ogloblina, M. Grofulović, L. Terraz, M. Lino da Silva, C. D. Pintassilgo, L. L. Alves, and O. Guaitella, “The case for in situ resource utilisation for oxygen production on Mars by non- equilibrium plasmas,” *Plasma Sources Sci. Technol.* **26**, 11LT01 (2017).
- ⁴⁸A. F. Silva, A. S. Morillo-Candas, A. Tejero-del-Caz, L. L. Alves, O. Guaitella, and V. Guerra, “A reaction mechanism for vibrationally cold CO₂ plasmas,” *Plasma Sources Sci. Technol.* (2020), 10.1088/1361-6595/abc818.
- ⁴⁹P. Ogloblina, A. S. Morillo-Candas, A. F. Silva, T. Silva, A. T. del Caz, L. L. Alves, O. Guaitella, and V. Guerra, “Mars in situ oxygen and propellant production by non-equilibrium plasmas,” *Plasma Sources Sci. Technol.* **30**, 065005 (2021).
- ⁵⁰G. Raposo, *Plasma in-situ production of fuel and oxygen on Mars*, Master’s thesis, Instituto Superior Técnico, Universidade de Lisboa, Portugal (2020).
- ⁵¹R. Snoeckx and A. Boagerts, “Plasma technology - a novel solution for CO₂ conversion?” *Chem. Soc. Rev.* **46**, 5805–5863 (2017).
- ⁵²M. Grofulović, T. Silva, B. L. M. Klarenaar, A. S. Morillo-Candas, O. Guaitella, R. Engeln, C. D. Pintassilgo, and V. Guerra, “Kinetic study of CO₂ plasmas under non-equilibrium conditions. II. Input of vibrational energy,” *Plasma Sources Sci. Technol.* **27**, 015009 (2018).
- ⁵³P. Ogloblina, A. Tejero-del-Caz, V. Guerra, and L. L. Alves, “Electron impact cross sections for carbon monoxide and their importance in the electron kinetics of CO₂–CO mixtures,” *Plasma Sources Sci. Technol.* **29**, 015002 (2020).
- ⁵⁴A. Starikovskiy and N. Aleksandrov, “Plasma-assisted ignition and combustion,” *Prog. Energy Combust. Sci.* **39**, 61–110 (2013).
- ⁵⁵P. Verma, O. D. Samuel, T. N. Verma, and G. Dwivedi, eds., *Advancement in Materials*,

- Manufacturing and Energy Engineering, Vol. I* (Springer, Singapore, 2022).
- ⁵⁶Y. Yin, T. Yang, Z. Li, E. Devid, D. Auerbach, and A. W. Kleyn, “CO₂ conversion by plasma: how to get efficient CO₂ conversion and high energy efficiency,” *Phys. Chem. Chem. Phys.* **23**, 7974–7987 (2021).
- ⁵⁷B. L. M. Klarenaar, R. Engeln, D. C. M. van den Bekerom, M. C. M. van de Sanden, A. S. Morillo-Candas, and O. Guaitella, “Time evolution of vibrational temperatures in a CO₂ glow discharge measured with infrared absorption spectroscopy,” *Plasma Sources Sci. Technol.* **26**, 115008 (2017).
- ⁵⁸A. S. Morillo-Candas, V. Guerra, and O. Guaitella, “Time evolution of the dissociation fraction in rf CO₂ plasmas: Impact and nature of back-reaction mechanisms,” *J. Phys. Chem. C* **124**, 17459–17475 (2020).
- ⁵⁹T. Silva, N. Britun, T. Godfroid, and R. Snyders, “Optical characterization of a microwave pulsed discharge used for dissociation of CO₂,” *Plasma Sources Sci. Technol.* **23**, 25009 (2014).
- ⁶⁰G. V. Pokrovskiy, N. A. Popov, and S. M. Starikovskaia, “Fast gas heating and kinetics of electronically excited states in a nanosecond capillary discharge in CO₂,” *Plasma Sources Sci. Technol.* **31**, 035010 (2022).
- ⁶¹M. Ceppelli, T. P. W. Salden, L. M. Martini, G. Dilecce, and P. Tosi, “Time-resolved optical emission spectroscopy in CO₂ nanosecond pulsed discharges,” *Plasma Sources Science and Technology* **30**, 115010 (2021).
- ⁶²C. A. Pavan and C. Guerra-Garcia, “Nanosecond pulsed discharge dynamics during passage of a transient laminar flame,” arXiv:2110.15423 [physics.plasm-ph] (2021).
- ⁶³G. M. Pokrovskiy, *Dissociation of carbon dioxide in pulsed plasma at high electric fields: role of energy exchange with electronically excited species*, Phd thesis, École Polytechnique - Institut Polytechnique de Paris (2021).
- ⁶⁴G. Chen, R. Snyders, and N. Britun, “CO₂ conversion using catalyst-free and catalyst-assisted plasma-processes: recent progress and understanding,” *J. CO₂ Util.* **49**, 101557 (2021).
- ⁶⁵M. Grofulović, B. L. M. Klarenaar, O. Guaitella, V. Guerra, and R. Engeln, “A rotational Raman study under non-thermal conditions in pulsed CO₂-N₂ and CO₂-O₂ glow discharges,” *Plasma Sources Sci. Technol.* **28**, 045014 (2019).
- ⁶⁶U. Kogelschatz, “Dielectric-barrier discharges: their history, discharge physics, and in-

- dustrial applications,” *Plasma Chem. Plasma Process.* **23**, 1–46 (2003).
- ⁶⁷I. Adamovich *et al*, “The 2017 plasma roadmap: low temperature plasma science and technology,” *J. Phys. D: Appl. Phys.* **50**, 323001 (2017).
- ⁶⁸T. Kimura, K. Ohe, and M. Nakamura, “Formation of dip structure of electron energy distribution function in diffused nitrogen plasmas,” *J. Phys. Soc. Japan* **67**, 3443–3449 (1998).
- ⁶⁹S. M. Starikovskaia, N. B. Anikin, S. V. Pancheshnyi, D. V. Zatsepin, and A. Y. Starikovskii, “Pulsed breakdown at high overvoltage: development, propagation and energy branching,” *Plasma Sources Sci. Technol.* **10**, 344–355 (2001).
- ⁷⁰C. Guerra-Garcia, M. Martinez-Sanchez, R. B. Miles, and A. Starikovskiy, “Localized pulsed nanosecond discharges in a counterflow nonpremixed flame environment,” *Plasma Sources Science and Technology* **24**, 055010 (2015).
- ⁷¹N. A. Popov, “Kinetics of plasma-assisted combustion: effect of non-equilibrium excitation on the ignition and oxidation of combustible mixtures,” *Plasma Sources Sci. Technol.* **25**, 043002 (2016).
- ⁷²M. S. Bak, S. K. Im, and M. Cappelli, “Nanosecond-pulsed discharge plasma splitting of carbon dioxide,” *IEEE Trans. Plasma Sci.* **43**, 1002–1007 (2015).
- ⁷³J. Maillard, T. Van den Biggelaar, E. Pannier, and C. O. Laux, “Time-resolved optical emission spectroscopy measurements of electron density and temperature in CO₂ nanosecond repetitively pulsed discharges,” in *AIAA SCITECH 2022 Forum* (2021).
- ⁷⁴M. Ceppelli, L. M. Martini, G. Dilecce, M. Scotoni, and P. Tosi, “Non-thermal rate constants of quenching and vibrational relaxation in the OH(A²Σ⁺, v' = 0, 1) manifold,” *Plasma Sources Sci. Technol.* **29**, 065019 (2020).
- ⁷⁵C. Montesano, S. Quercetti, L. M. Martini, G. Dilecce, and P. Tosi, “The effect of different pulse patterns on the plasma reduction of CO₂ for a nanosecond discharge,” *J. CO₂ Util.* **39**, 101157 (2020).
- ⁷⁶I. Gulko, E. R. Jans, C. Richards, S. Raskar, X. Yang, D. C. M. van den Bekerom, and I. V. Adamovich, “Nanosecond-pulsed discharge plasma splitting of carbon dioxide,” *Plasma Sources Sci. Technol.* **29**, 104002 (2020).
- ⁷⁷E. Plönjes, P. Palm, W. Lee, W. R. Lempert, and I. V. Adamovich, “Radio frequency energy coupling to high-pressure optically pumped nonequilibrium plasmas,” *J. Appl. Phys.* **89**, 5911–5918 (2001), <https://doi.org/10.1063/1.1359755>.

- ⁷⁸A. R. Gibson, Z. Donkó, L. Alelyani, L. Bischoff, G. Hübner, J. Bredin, S. Doyle, I. Korolov, K. Niemi, and T. Mussenbrock, “Disrupting the spatio-temporal symmetry of the electron dynamics in atmospheric pressure plasmas by voltage waveform tailoring,” *Plasma Sources Sci. Technol.* **28**, 01LT01 (2019).
- ⁷⁹K. Frederickson, Y.-C. Hung, W. R. Lempert, and I. V. Adamovich, “Control of vibrational distribution functions in nonequilibrium molecular plasmas and high-speed flows,” *Plasma Sources Sci. Technol.* **26**, 014002 (2017).
- ⁸⁰X. Mao, Q. Chen, A. C. Rousso, T. Y. Chen, and Y. Ju, “Effects of controlled nonequilibrium excitation on H₂/O₂/He ignition using a hybrid repetitive nanosecond and DC discharge,” *Combust. Flame* **206**, 522–535 (2019).
- ⁸¹X. Mao, A. C. Rousso, Q. Chen, and Y. Ju, “Numerical modeling of ignition enhancement of CH₄/O₂/He mixtures using a hybrid repetitive nanosecond and dc discharge,” *Proc. Combust. Inst.* **37**, 5545–5552 (2019).
- ⁸²B. Ashford and X. Tu, “Non-thermal plasma technology for the conversion of CO₂,” *CRGSC* **3**, 45–49 (2017).
- ⁸³B. Ashford, Y. Wang, C.-K. Poh, L. Chen, and X. Tu, “Plasma-catalytic conversion of CO₂ to CO over binary metal oxide catalysts at low temperatures,” *Appl. Catal. B* **276**, 119110 (2020).
- ⁸⁴S. Mori and L. L. Tun, “Synergistic CO₂ conversion by hybridization of dielectric barrier discharge and solid oxide electrolyser cell,” *Plasma Process. Polym.* **14**, 1–6 (2017).
- ⁸⁵G. B. Hoflund, “Oxygen transport through high-purity, large-grain Ag,” *J. Mater. Res.* **3**, 1378–1384 (1988).
- ⁸⁶P. Vernoux, L. Lizarraga, M. N. Tsampas, F. M. Sapountzi, A. De Lucas-Consuegra, J. L. Valverde, S. Souentie, C. G. Vayenas, D. Tsiplakides, S. Balomenou, and E. A. Baranova, “Ionically conducting ceramics as active catalyst supports,” *Chem. Rev.* **113**, 8192–8260 (2013).
- ⁸⁷A. Azim Jais, S. Muhammed Ali, M. Anwar, M. Rao Somalu, A. Muchtar, W. N. R. Wan Isahak, C. Yong Tan, R. Singh, and N. P. Brandon, “Enhanced ionic conductivity of scandia-ceria-stabilized-zirconia (10Sc1CeSZ) electrolyte synthesized by the microwave-assisted glycine nitrate process,” *Ceramics International* **43**, 8119–8125 (2017).
- ⁸⁸A. Arratibel Plazaola, A. Cruellas Labella, Y. Liu, N. Badiola Porras, D. A. Pacheco Tanaka, M. V. Sint Annaland, and F. Gallucci, “Mixed ionic-electronic conduct-

- ing membranes (miec) for their application in membrane reactors: A review,” *Processes* **7** (2019), 10.3390/pr7030128.
- ⁸⁹W. Meulenberg, F. Schulze-Küppers, W. Deibert, T. Van Gestel, and S. Baumann, “Keramische membranen: Materialien – bauteile – potenzielle anwendungen,” *Chem. Ing. Tech.* **91**, 1091–1100 (2019), wiley deal.
- ⁹⁰S. Hashim, A. Mohamed, and S. Bhatia, “Oxygen separation from air using ceramic-based membrane technology for sustainable fuel production and power generation,” *Renew. Sustain. Energy Rev.* **15**, 1284–1293 (2011).
- ⁹¹M. Rohnke, J. Janek, J. A. Kilner, and R. J. Chater, “Surface oxygen exchange between yttria-stabilised zirconia and a low-temperature oxygen rf-plasma,” *Solid State Ionics* **166**, 89–102 (2004).
- ⁹²R. A. Outlaw, “O₂ and CO₂ glow-discharge-assisted oxygen transport through Ag,” *J. Appl. Phys.* **68**, 1002–1004 (1990).
- ⁹³D. Wu, R. A. Outlaw, and R. L. Ash, “Glow-discharge enhanced permeation of oxygen through silver,” *J. Appl. Phys.* **74**, 4990–4994 (1993).
- ⁹⁴D. Wu, R. A. Outlaw, and R. L. Ash, “Extraction of oxygen from CO₂ using glow-discharge and permeation techniques,” *J. Vac. Sci. Technol. A* **14**, 408–414 (1996).
- ⁹⁵D. Premathilake, R. A. Outlaw, R. A. Quinlan, and C. E. Byvik, “Oxygen generation by carbon dioxide glow discharge and separation by permeation through ultrathin silver membranes,” *Earth and Space Science* (2019), 10.1029/2018EA000521.
- ⁹⁶Q. Zheng, Y. Xie, J. Tan, Z. Xu, P. Luo, T. Wang, Z. Liu, F. Liu, K. Zhang, Z. Fang, G. Zhang, and W. Jin, “Coupling of dielectric barrier discharge plasma with oxygen permeable membrane for highly efficient low-temperature permeation,” *J. Membr. Sci.* **641**, 119896 (2022).
- ⁹⁷S. O. Steinmüller, M. Rohnke, and J. Janek, “Low pressure oxygen direct current discharges with ion conducting yttria stabilized zirconia electrodes,” *Solid State Ion.* **245–246**, 24–32 (2013).
- ⁹⁸A. Pandiyani, V. Di Palma, V. Kyriakou, W. M. M. Kessels, M. Creatore, M. C. van de Sanden, and M. N. Tsampas, “Enhancing the electrocatalytic activity of redox stable perovskite fuel electrodes in solid oxide cells by atomic layer-deposited Pt nanoparticles,” *ACS Sustainable Chem. Eng.* **8**, 12646–12654 (2020).
- ⁹⁹E. V. Kustova, E. A. Nagnibeda, and I. Armenise, “Vibrational-chemical kinetics in mars

- entry problems,” *The Open Plasma Physics Journal* **7**, 76–87 (2014).
- ¹⁰⁰J. Annaloro and A. Bultel, “Vibrational and electronic collisional-radiative model in CO₂-N₂-Ar mixtures for mars entry problems,” *Phys. Plasmas* **26**, 103505 (2019).
- ¹⁰¹E. Kustova and M. Mekhonoshina, “Multi-temperature vibrational energy relaxation rates in CO₂,” *Phys. Fluids* **32**, 096101 (2020).
- ¹⁰²A. Kosareva, O. Kunova, E. Kustova, and E. Nagnibeda, “Four-temperature kinetic model for CO₂ vibrational relaxation,” *Phys. Fluids* **33**, 016103 (2021).
- ¹⁰³T. Kozák and A. Bogaerts, “Splitting of CO₂ by vibrational excitation in non-equilibrium plasmas: a reaction kinetics model,” *Plasma Sources Science and Technology* **23**, 045004 (2014).
- ¹⁰⁴L. D. Pietanza, G. Colonna, G. D’Ammando, A. Laricchiuta, and M. Capitelli, “Vibrational excitation and dissociation mechanisms of CO₂ under non-equilibrium discharge and post-discharge conditions,” *Plasma Sources Sci. Technol.* **24**, 042002 (2015).
- ¹⁰⁵L. D. Pietanza, G. Colonna, and M. Capitelli, “Non-equilibrium plasma kinetics of reacting CO: an improved state to state approach,” *Plasma Sources Sci. Technol.* **26**, 125007 (2017).
- ¹⁰⁶L. D. Pietanza, G. Colonna, and M. Capitelli, “Electron energy and vibrational distribution functions of carbon monoxide in nanosecond atmospheric discharges and microsecond afterglows,” *J. Plasma Phys.* **83**, 725830603 (2017).
- ¹⁰⁷T. Silva, M. Grofulović, B. L. M. Klarenaar, O. Guaitella, R. Engeln, C. D. Pintassilgo, and V. Guerra, “Kinetic study of CO₂ plasmas under non-equilibrium conditions. I. Relaxation of vibrational energy,” *Plasma Sources Sci. Technol.* **27**, 015019 (2018).
- ¹⁰⁸L. Terraz, T. Silva, A. Morillo-Candas, O. Guaitella, A. Tejero-del-Caz, L. L. Alves, and V. Guerra, “Influence of N₂ on the CO₂ vibrational distribution function and dissociation yield in non-equilibrium plasmas,” *J. Phys. D: Appl. Phys.* **53**, 094002 (2020).
- ¹⁰⁹T. Silva, M. Grofulović, L. Terraz, C. D. Pintassilgo, and V. Guerra, “Dynamics of gas heating in the afterglow of pulsed CO₂ and CO₂-N₂ glow discharges at low pressure,” *Plasma Chem. Plasma Process.* (2020), 10.1007/s11090-020-10061-7.
- ¹¹⁰T. Silva, A. S. Morillo-Candas, O. Guaitella, and V. Guerra, “Modeling the time evolution of the dissociation fraction in low-pressure CO₂ plasmas,” *J. CO₂ Util.* **53**, 101719 Contents (2021).
- ¹¹¹G. V. Naidis and N. Y. Babaeva, “Modeling of repetitively pulsed low-pressure CO₂

- discharges,” *Phys. Plasmas* **29**, 044501 (2022).
- ¹¹²A. Tejero-del-Caz, V. Guerra, D. Gonçalves, M. Lino da Silva, L. Marques, N. Pinhão, C. D. Pintassilgo, and L. L. Alves, “The LisOn KInetics Boltzmann solver,” *Plasma Sources Sci. Technol.* **28**, 043001 (2019).
- ¹¹³Q. Hong, M. Bartolomei, C. Coletti, A. Lombardi, Q. Sun, and F. Pirani, “Vibrational energy transfer in CO+N₂ collisions: A database for V–V and V–T/R quantum-classical rate coefficients,” *Molecules* **26**, 7152 (2021).
- ¹¹⁴A. K. Kurnosov, A. P. Napartovich, S. L. Shnyrev, and M. Cacciatore, “A database for V–V state-to-state rate constants in N₂-N₂ and N₂-CO collisions in a wide temperature range: dynamical calculations and analytical approximations,” *Plasma Sources Sci. Technol.* **19**, 045015 (2010).
- ¹¹⁵M. López-Puertas, R. Rodrigo, J. J. López-Moreno, and F. W. Taylor, “A non-LTE radiative transfer model for infrared bands in the middle atmosphere. II. CO₂ (2.7 and 4.3 μm) and water vapour (6.3 μm) bands and N₂(1) and O₂(1) vibrational levels,” *J. Atmospheric Terr. Phys.* **48**, 749–746 (1986).
- ¹¹⁶M. Capitelli, C. M. Ferreira, B. F. Gordiets, and A. I. Osipov, *Plasma Kinetics in Atmospheric Gases* (Springer, Berlin, 2000).
- ¹¹⁷G. D. Billing, “Vibration-vibration and vibration-translation energy transfer, including multiquantum transitions in atom-diatom and diatom-diatom collisions,” in *Nonequilibrium Vibrational Kinetics*, edited by M. Capitelli (Springer-Verlag, Berlin Heidelberg, 1986) Chap. 6.
- ¹¹⁸V. Guerra, A. Tejero-del-Caz, C. D. Pintassilgo, and L. L. Alves, “Modelling N₂-O₂ plasmas: volume and surface kinetics,” *Plasma Sources Sci. Technol.* **28**, 073001 (2019).
- ¹¹⁹K. Kutasi, V. Guerra, and P. Sá, “Theoretical insight into Ar–O₂ surface-wave microwave discharges,” *J. Phys. D: Appl. Phys.* **43**, 175201 (2010).
- ¹²⁰M. Grofulović, L. L. Alves, and V. Guerra, “Electron-neutral scattering cross sections for CO₂: a complete and consistent set and an assessment of dissociation,” *J. Phys. D: Appl. Phys.* **49**, 395207 (2016).
- ¹²¹L. D. Pietanza, G. Colonna, G. D’Ammando, A. Laricchiuta, and M. Capitelli, “Electron energy distribution functions and fractional power transfer in “cold” and excited CO₂ discharge and post discharge conditions,” *Phys. Plasmas* **23**, 013515 (2016).
- ¹²²Y. Gorbanev, E. Vervloessem, A. Nikiforov, and A. Bogaerts, “Nitrogen fixation with

- water vapor by nonequilibrium plasma: toward sustainable ammonia production,” *ACS Sustainable Chem. Eng.* **8**, 2996–3004 (2020).
- ¹²³K. H. Rouwenhorst, Y. Engelmann, K. van’t Veer, R. S. Postma, A. Bogaerts, and L. Leferts, “Plasma-driven catalysis: green ammonia synthesis with intermittent electricity,” *Green chemistry* **22**, 6258–6287 (2020).
- ¹²⁴S. Kelly and A. Bogaerts, “Nitrogen fixation in an electrode-free microwave plasma,” *Plasma Sources Sci. Technol.* **5**, 3006–3030 (2021).
- ¹²⁵A. Chatain, M. Jiménez-Redondo, L. Vettier, O. Guaitella, N. Carrasco, L. L. Alves, L. Marques, and G. Cernogora, “N₂-H₂ capacitively coupled radio-frequency discharges at low pressure. Part I. Experimental results: effect of the H₂ amount on electrons, positive ions and ammonia formation,” *Plasma Sources Sci. Technol.* **29**, 085019 (2020).
- ¹²⁶M. Jiménez-Redondo, A. Chatain, O. Guaitella, G. Cernogora, N. Carrasco, L. L. Alves, and L. Marques, “N₂-H₂ capacitively coupled radio-frequency discharges at low pressure: II. Modeling results: the relevance of plasma-surface interaction,” *Plasma Sources Sci. Technol.* **29**, 085023 (2020).
- ¹²⁷R. Antunes, R. Steiner, C. Romero-Muñiz, K. Soni, L. Marot, and E. Meyer, “Plasma-assisted catalysis of ammonia using tungsten at low pressures: A parametric study,” *ACS Appl. Energy Mater.* **4**, 4385–4394 (2021).
- ¹²⁸S. Finch, A. Samuel, and G. P. Lane, *Lockhart and wiseman’s crop husbandry including grassland* (Elsevier, 2014).
- ¹²⁹B. S. Patil, F. Peeters, G. J. van Rooij, J. Medrano, F. Gallucci, J. Lang, Q. Wang, and V. Hessel, “Plasma assisted nitrogen oxide production from air: Using pulsed powered gliding arc reactor for a containerized plant,” *AIChE Journal* **64**, 526–537 (2018).
- ¹³⁰M. A. Malik, “Nitric oxide production by high voltage electrical discharges for medical uses: a review,” *Plasma Chem. Plasma Process.* **36**, 737–766 (2016).
- ¹³¹B. Mutel, O. Dessaux, and P. Goudmand, “Energy cost improvement of the nitrogen oxides synthesis in a low pressure plasma,” *Revue de physique appliquée* **19**, 461–464 (1984).
- ¹³²B. Eliasson, M. Hirth, and U. Kogelschatz, “Ozone synthesis from oxygen in dielectric barrier discharges,” *J. Phys. D: Appl. Phys.* **20**, 1421–1437 (1987).
- ¹³³U. Kogelschatz, B. Eliasson, and M. Hirth, “Ozone generation from oxygen and air: discharge physics and reaction mechanisms,” *Ozone-Sci. Eng.* **10**, 367–378 (1988).

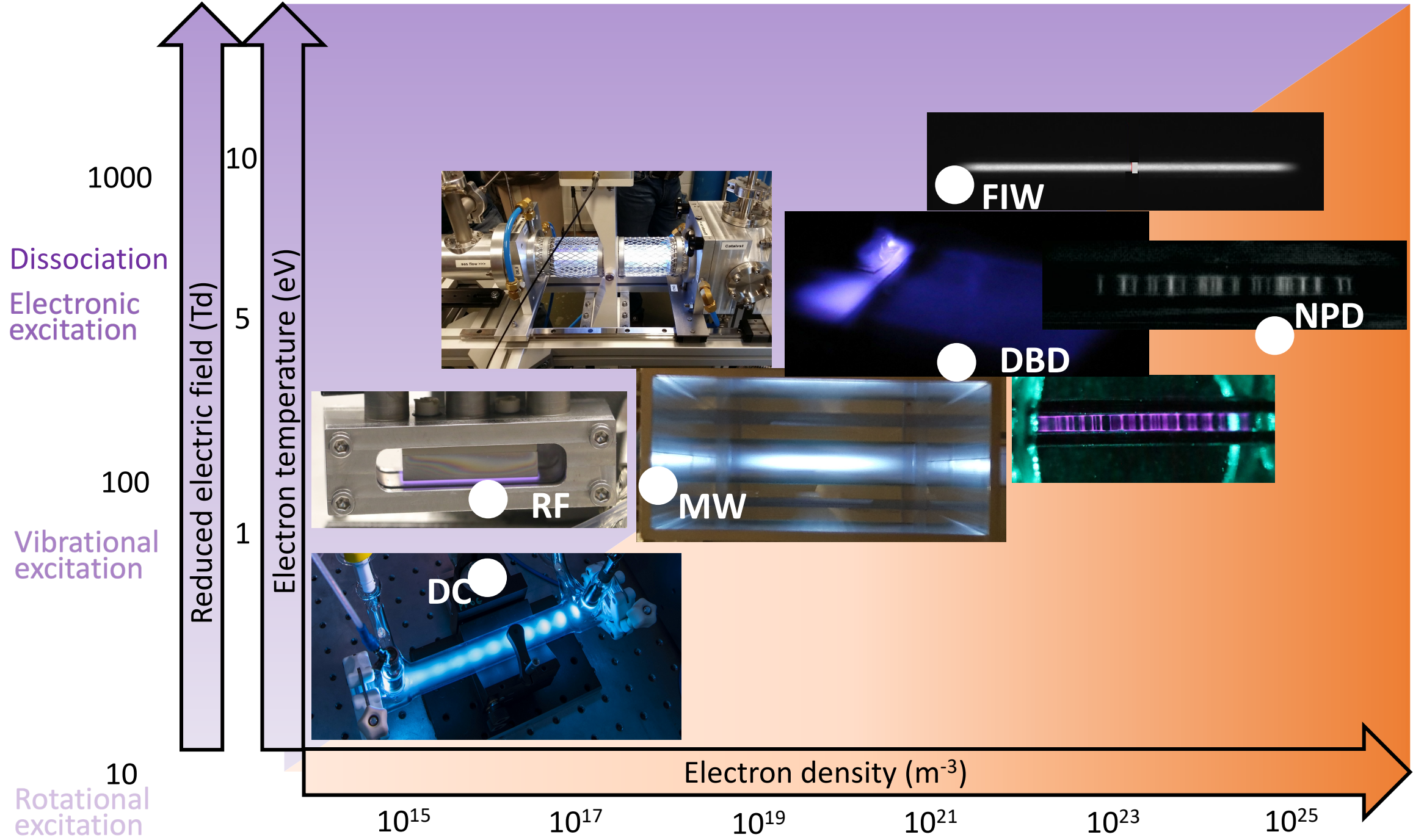
- ¹³⁴C. Ayrault, J. Barrault, N. Blin-Simi, , F. Jorand, S. Pasquiers, A. Rousseau, and J. Tatibouët, “Oxidation of 2-heptanone in air by a DBD-type plasma generated within a honeycomb monolith supported Pt-based catalyst,” *Catalysis Today* **89**, 75–81 (2004).
- ¹³⁵U. Roland, F. Holzer, and F.-D. Kopinke, “Improved oxidation of air pollutants in a non-thermal plasma,” *Catalysis Today* **73**, 315–323 (2002).
- ¹³⁶A. Bogaerts, X. Tu, J. C. Whitehead, G. Centi, L. Lefferts, O. Guaitella, F. Azzolina-Jury, H.-H. Kim, A. B. Murphy, W. F. Schneider, *et al.*, “The 2020 plasma catalysis roadmap,” *Journal of physics D: applied physics* **53**, 443001 (2020).
- ¹³⁷M. Nagatsu, F. Terashita, H. Nonaka, L. Xu, T. Nagata, and Y. Koide, “Effects of oxygen radicals in low-pressure surface-wave plasma on sterilization,” *Appl. Phys. Lett.* **86**, 211502 (2005).
- ¹³⁸S. Ognier, D. Iya-sou, C. Fourmond, and S. Cavadias, “Analysis of mechanisms at the plasma–liquid interface in a gas–liquid discharge reactor used for treatment of polluted water,” *Plasma Chem. Plasma Proc.* **29**, 261–273 (2009).
- ¹³⁹A. Bultel and J. Annaloro, “Elaboration of collisional–radiative models for flows related to planetary entries into the Earth and Mars atmospheres,” *Plasma Sources Sci. Technol.* **22**, 025008 (2013).
- ¹⁴⁰A. Bourdon, J. Annaloro, A. Bultel, M. Capitelli, G. Colonna, A. Guy, T. E. Magin, A. Munafó, M. Y. Perrin, and L. D. Pietanza, “Reduction of state-to-state to macroscopic models for hypersonics,” *Open Plasma Phys. J.* **7**, 60–75 (2014).
- ¹⁴¹B. Gordiets and A. Ricard, “Production of N, O and NO in N₂-O₂ flowing discharges,” *Plasma Sources Sci. Technol.* **2**, 158–163 (1993).
- ¹⁴²B. F. Gordiets and C. M. Ferreira, “Self-consistent modeling of volume and surface processes in air plasma,” *AIAA Journal* **36**, 1643–1651 (1998).
- ¹⁴³P. Coche, V. Guerra, and L. L. Alves, “Microwave air plasmas in capillaries at low pressure I. Self-consistent modeling,” *J. Phys. D: Appl. Phys.* **49**, 235207 (2016).
- ¹⁴⁴C. D. Pintassilgo, J. Loureiro, and V. Guerra, “Modelling of a N₂-O₂ flowing afterglow for plasma sterilization,” *J. Phys. D: Appl. Phys.* **38**, 417 (2005).
- ¹⁴⁵V. Guerra and J. Loureiro, “Self-consistent electron and heavy-particle kinetics in a low pressure N₂-O₂ glow discharge,” *Plasma Sources Sci. Technol.* **6**, 373–385 (1997).
- ¹⁴⁶C. D. Pintassilgo, O. Guaitella, and A. Rousseau, “Heavy species kinetics in low-pressure dc pulsed discharges in air,” *Plasma Sources Sci. Technol.* **18**, 025005 (2009).

- ¹⁴⁷J. Loureiro and C. M. Ferreira, “Coupled electron energy and vibrational distribution functions in stationary N₂ discharges,” *J. Phys. D: Appl. Phys.* **19**, 17–35 (1986).
- ¹⁴⁸B. F. Gordiets, C. M. Ferreira, V. L. Guerra, J. M. A. H. Loureiro, J. Nahorny, D. Pagnon, M. Touzeau, and M. Vialle, “Kinetic model of a low-pressure N₂-O₂ flowing glow discharge,” *IEEE Trans. on Plasma. Sci.* **23**, 750–767 (1995).
- ¹⁴⁹V. Guerra and J. Loureiro, “Non-equilibrium coupled kinetics in stationary N₂-O₂ discharges,” *J. Phys. D: Appl. Phys.* **28**, 1903–1918 (1995).
- ¹⁵⁰G. Dilecce and S. De Benedictis, “Experimental studies on elementary kinetics in N₂-O₂ pulsed discharges,” *Plasma Sources Sci. Technol.* **8**, 266–278 (1999).
- ¹⁵¹V. Guerra, “Analytical model of heterogeneous atomic recombination on silicalike surfaces,” *IEEE Trans. Plasma Sci.* **35**, 1397–1412 (2007).
- ¹⁵²M. Castillo, V. Herrero, I. Mendez, and I. Tanarro, “Spectrometric and kinetic study of a modulated glow air discharge,” *Plasma Sources Sci. Technol.* **13**, 343–350 (2004).
- ¹⁵³M. Castillo, I. Mendéz, A. M. Islyaikin, V. J. Herrero, and I. Tanarro, “Low-pressure DC air plasmas. investigation of neutral and ion chemistry,” *J. Phys. Chem. A* **109**, 6255–6263 (2005).
- ¹⁵⁴V. Guerra, D. Marinov, O. Guaitella, and A. Rousseau, “NO oxidation on plasma pre-treated Pyrex: the case for a distribution of reactivity of adsorbed O atoms,” *J. Phys. D: Appl. Phys.* **47**, 224012 (2014).
- ¹⁵⁵O. Guaitella, M. Hübner, S. Welzel, D. Marinov, J. Röpcke, and A. Rousseau, “Evidence for surface oxidation on Pyrex of NO into NO₂ by adsorbed O atoms,” *Plasma Sources Sci. Technol.* **19**, 45026 (2010).
- ¹⁵⁶G. D. Stancu, O. Leroy, P. Coche, K. Gadonna, V. Guerra, T. Minea, and L. L. Alves, “Microwave air plasmas in capillaries at low pressure: II. Experimental investigation,” *J. Phys. D: Appl. Phys.* **49**, 435202 (2016).
- ¹⁵⁷R. A. B. Zijlmans, S. Welzel, O. Gabriel, G. Yagci, J. H. van Helden, J. Röpcke, D. C. Schram, and R. Engeln, “Experimental study of surface contributions to molecule formation in a recombining N₂/O₂ plasma,” *J. Phys. D: Appl. Phys.* **43**, 115204 (2010).
- ¹⁵⁸H. Patel, R. K. Sharma, V. Kyriakou, A. Pandiyan, S. Welzel, M. C. van de Sanden, and M. N. Tsampas, “Plasma-activated electrolysis for cogeneration of nitric oxide and hydrogen from water and nitrogen,” *ACS Energy Lett.* **4**, 2091–2095 (2019).
- ¹⁵⁹J. Pelletier and A. Anders, “Plasma-based ion implantation and deposition: a review of

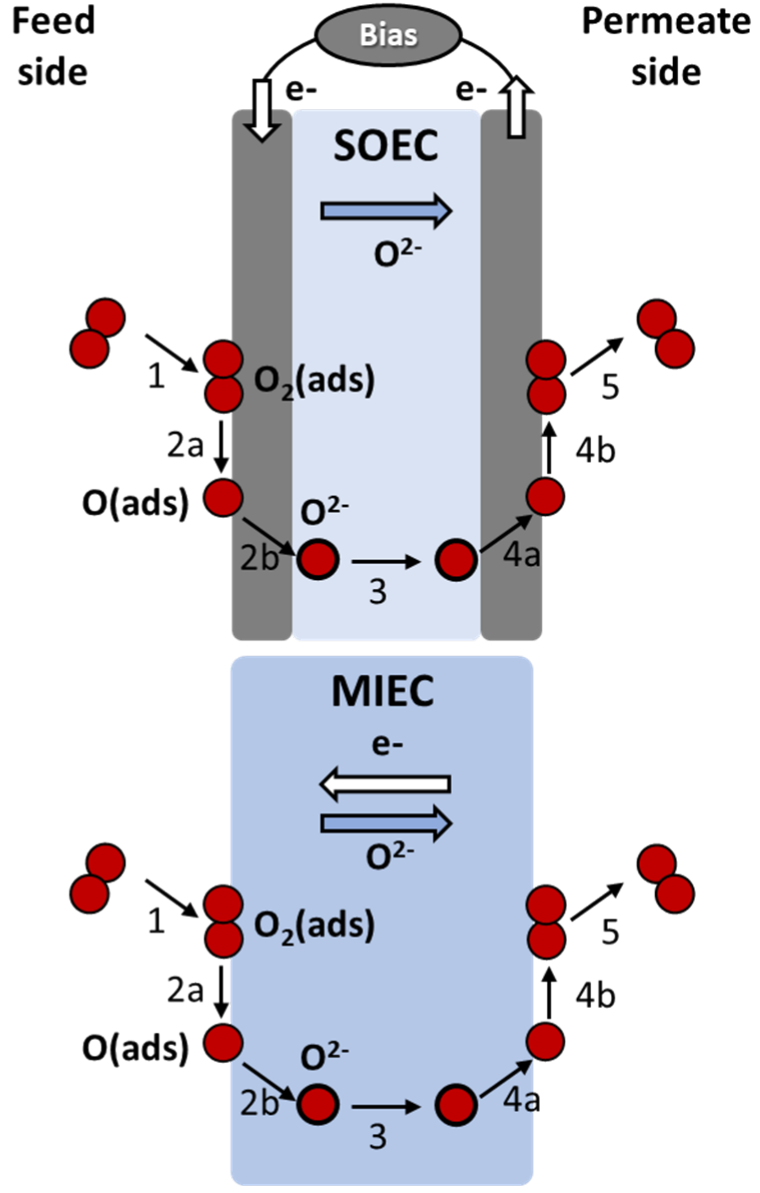
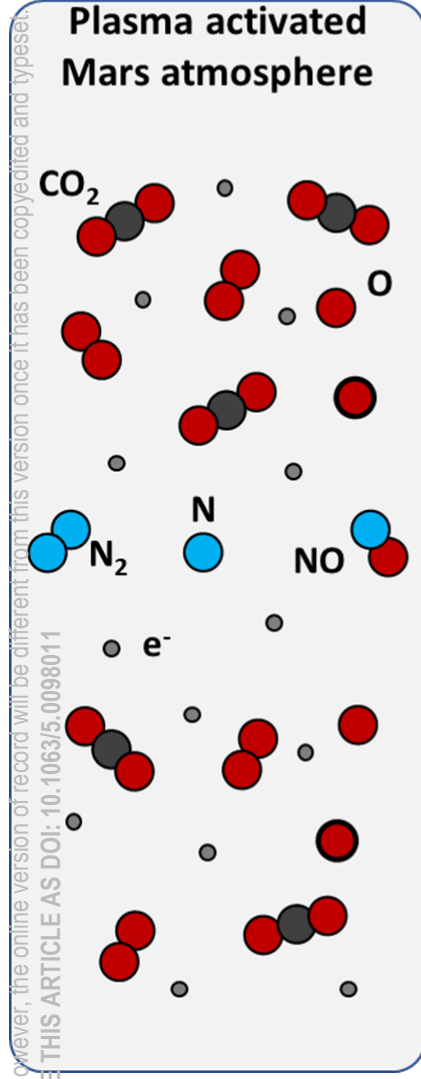
This is the author's peer reviewed, accepted manuscript. However, the online version of record will be different from this version once it has been copyedited and typeset.
PLEASE CITE THIS ARTICLE AS DOI: 10.1063/5.0098011

- physics, technology, and applications,” *IEEE Trans. Plasma Sci.* **33**, 1944 – 1959 (2005).
- ¹⁶⁰S. N. Bathgate, M. M. M. Bilek, and D. R. McKenzie, “Electrodeless plasma thrusters for spacecraft: a review,” *Plasma Sci. Technol.* **19**, 083001 (2017).
- ¹⁶¹A. Bapat, P. B. Salunkhe, and A. V. Patil, “Hall-effect thrusters for deep-space missions: A review,” *IEEE Trans. Plasma Sci.* **50**, 189–202 (2022).
- ¹⁶²T. P. Polsgrove, T. K. Percy, M. Rucker, and H. D. Thomas, “Update to mars ascent vehicle design for human exploration,” in *2019 IEEE Aerospace Conference* (2019) pp. 1–15.
- ¹⁶³R. K. Sharma, H. Patel, U. Mushtaq, V. Kyriakou, G. Zafeiropoulos, F. Peeters, S. Welzel, M. C. M. van de Sanden, and M. N. Tsampas, “Plasma activated electrochemical ammonia synthesis from nitrogen and water,” *ACS Energy Letters* **6**, 313–319 (2021).

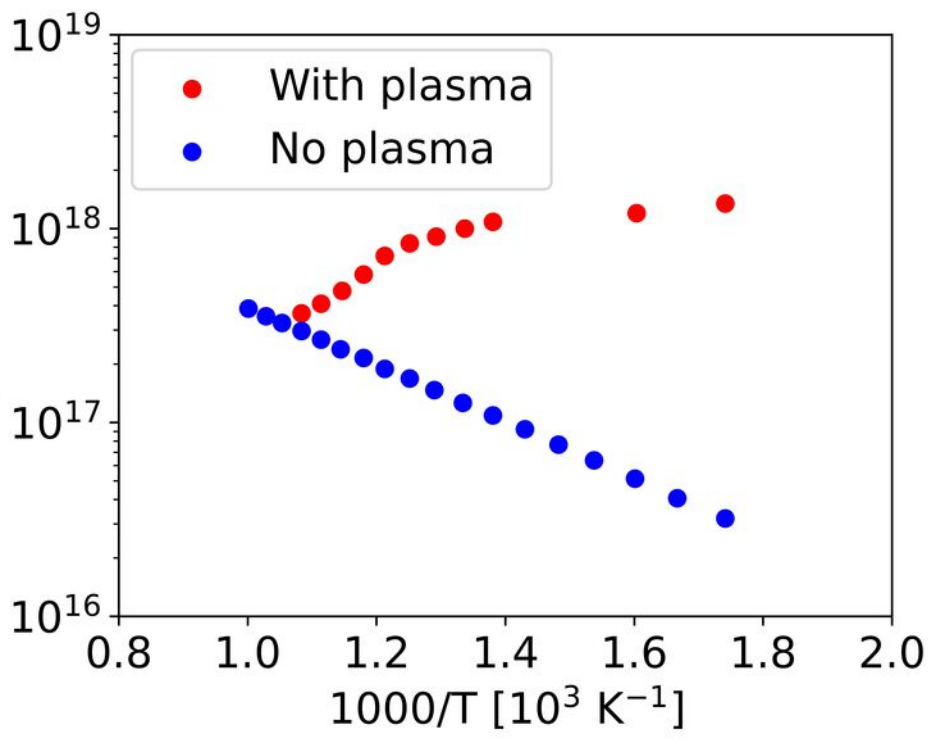
This is the author's peer reviewed, accepted manuscript. However, the online version of record will be different from this version once it has been copyedited and typeset.
PLEASE CITE THIS ARTICLE AS DOI: 10.1063/5.0098011



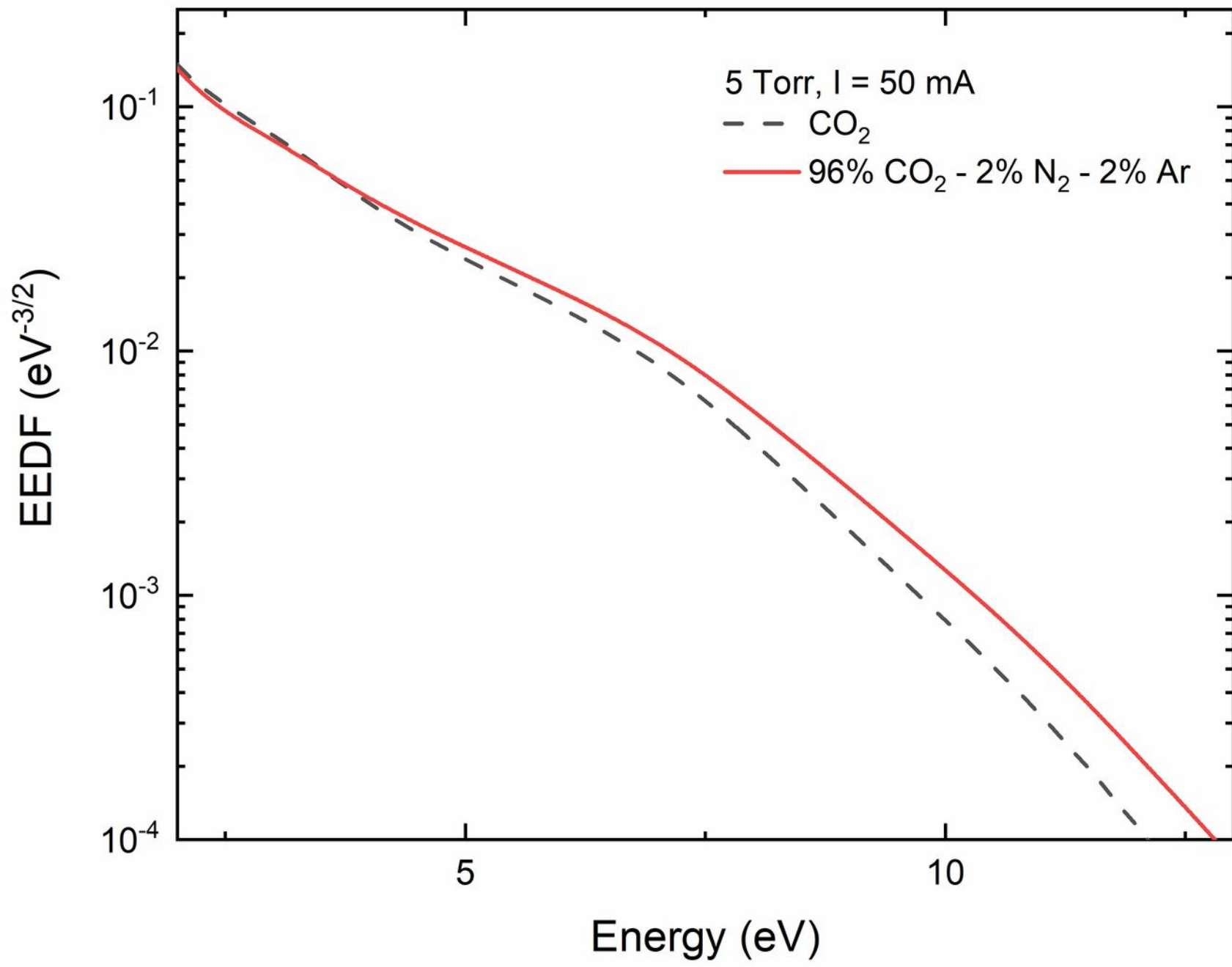
This is the author's peer reviewed, accepted manuscript. However, the online version of record will be different from this version once it has been copyedited and typeset.
PLEASE CITE THIS ARTICLE AS DOI: 10.1063/5.0098011



This is the author's peer reviewed, accepted manuscript. However, the online version of record will be different from this version once it has been copyedited and typeset.
PLEASE CITE THIS ARTICLE AS DOI: 10.1063/5.0098011



This is the author's peer reviewed, accepted manuscript. However, the online version of record will be different from this version once it has been copyedited and typeset.
PLEASE CITE THIS ARTICLE AS DOI: 10.1063/5.0098011



This is the author's peer reviewed, accepted manuscript. However, the online version of record will be different from this version once it has been copyedited and typeset.

PLEASE CITE THIS ARTICLE AS DOI: 10.1063/5.0098011

